Pharmacological characterization

of the odorant receptor MsextaOR-2

Diploma Thesis

Max-Planck-Institut
für chemische Ökologie

Max-Planck-Institut für chemische Ökologie

Abteilung Evolutionäre Neuroethologie

UNIKASSEL
VERSITÄT

Natur Technik Kultur Gesellschaft

In cooperation with

Universität Kassel

Fachbereich 10 Naturwissenschaften

Abteilung Tierphysiologie Kassel

Submitted by

Sarah Körte

Kassel, 29. Mai 2013

Referee:

Prof. Dr. Monika Stengl

Universität Kassel

Abteilung Tierphysiologie, FB 10 Naturwissenschaften

Heinrich-Plett-Straße 40

34132 Kassel

PD Dr. Dieter Wicher

Max-Planck-Institut für chemische Ökologie

Abteilung evolutionäre Neuroethologie

Hans-Knoll-Straße 8

07745 Jena

Table of content

List of abbreviations

AC	Adenylyl cyclase
AOX	Aldehyde oxidase
ATP	Adenosine triphosphate
BAL	E10, Z12 hexadecadienal
CaM	Calmodulin
cAMP	Cyclic adenosine monophosphate
cGMP	Cyclic guanosine monophosphate
CHO	Chinese hamster ovaries
CICR	Calcium-induced calcium release
CLSM	Confocal laser scanning microscopy
DAG	Diacylglycerol
EDTA	Ethylenediaminetetraacetic acid
ER	Endoplasmic reticulum
FACS	Fluorescence activated cell sorting
FCS	Fetal calf serum
GC	Guanylate cyclase
HEK	Human embryonic kidney
HBSS	Hank's balanced salt solution
HEPES	N-[2-hydroxyethyle]piperazine-N'-[2-ethanesulfonic acid]
IP_3	Inositol-1,4,5-triphosphate
OBP	Odorant-binding protein
OR	Odorant receptor
Orco	Odorant receptor co-receptor
ORN	Odorant receptor neuron
NGS	Normal goat serum
PBS	Phosphate buffered saline
PBP	Pheromone-binding protein
PIP_2	Phosphatidylinositol 4,5-bisphosphate
PMCA	Plasma membrane Ca^{2+}-ATPase
PKA	Protein kinase A

PKC	Protein kinase C
ROI	Regions of interest
RT	Room temperature
RyR	Ryanodine receptors
SERCA	Sarco endoplasmic reticular Ca^{2+}-ATPase
SES	Standard external solution
SNMP	Sensory neuron membrane protein

1 Introduction

1.1 Olfaction

In an insect's life perception of volatile compounds via the sense of smell, i.e. olfaction, and the corresponding genetically determined or learned behavior is crucial for survival of the individual and its entire population. The environment of insects is enriched with odorant molecules, from the odor blend of food sources and oviposition sites to repellent odorants or species-specific semiochemical mixtures. Multifarious as well as hardly discriminable stimuli have to be identified, evaluated and related in a context-depending manner. Due to these high requirements, insects evolved a complex system for olfactory chemoreception, whose sophistication and sensitivity is subject of ongoing research. As the detection of airborne, chemical cues via specialized chemosensory receptors has a vital importance for insects, manipulation of their olfactory system provides an opportunity to control deleterious behavior of agriculture pest species or the spreading of insect-borne diseases (Zwiebel & Takken, 2004; Syed & Leal, 2008; Ditzen et al., 2008; Jones et al., 2011). A starting point for this approach is an insect's distinct sensitivity for volatile cues related to intraspecific communication. Odor blends allowing for an exchange of information between individuals of the same species are called pheromones. While single pheromone components of closely related insect species can be identical, the compounds concentration ratio is unique for only one species. Pheromones, attracting conspecific partners and initiating mating behavior, were first identified by the German biochemist and Noble price winner A. Butenandt along with his colleagues, 1959, in the silkmoth *Bombyx mori* (Butenandt et al, 1959). Isolation and subsequent syntheses of the silkmoth's sex-pheromone established a basis for pioneering behavioral and electrophysiological studies in the field of insect olfaction. *B. mori* has been domesticated from its wild type *Bombyx mandarina* thousands of years ago. During the process of domestication amongst others the insect lost its ability of flight and its physiology changed, with the result that they entirely rely on human care in order to survive. In contrast to *B. mori*, the hawkmoth *Manduca sexta*, as another representative of the order Lepidoptera, has an ecological and agricultural relevance. This sphingid moth exhibits a complex behavior, has an exceedingly specific as well as sensitive olfactory sense and a relatively short generation time for a highly-developed organism. Characteristics like these made *M. sexta* a

popular model system in animal physiology, with a substantial amount of data available in the field of biochemistry, ecology, ethology, neurobiology and morphology (Hildebrand, 1995). Although work on *M. sexta* also greatly promoted the progress of elucidating the mechanisms underlying insect olfaction, little is known about the events following ligand binding to olfactory chemosensory receptors and leading to an odor or pheromone response.

1.2 Model organism *Manduca sexta*

The nocturnal sphingidae *M. sexta* populates wide, arid areas in North and Central America, where the moth is a dreaded pest species in agriculture. Caterpillars of this hawkmoth feed on various solanaceous plants and cause their defoliation, while they store and secrete the plants neurotoxin nicotine. Preferred host plants of *M. sexta*'s larvae belong to the genus Nicotiana, therefore larvae of this species are also commonly known as tobacco hornworms. Adults are colored dull gray to gray brown and exhibit six, matched, yellow to orange colored dots on the dorsal side of their abdomen. The bifid wings of full-grown *M. sexta* individuals measure about 120 mm across. They enable the hawkmoth, together with their exceedingly long proboscis, to hover while feeding on nectar from flowers such as *Datura wrightii* or *Nicotiana attenuata*. Field observations suggest life spans of adult *M. sexta* individuals up to 50 days. Female and male adults can be distinguished due to sexual dimorphism. Male hawkmoths possess claspers for mating at their terminal segments. Moreover, their antennae are broad and keyhole-like shaped while antennae from females are cylindrical in cross section (Sanes & Hildebrand, 1976; Keil, 1989). In the early hours of night female *M. sexta* start “calling” for males (Sasaki & Riddiford, 1984; Woods & Stevenson, 1996). After the females have been mated, they start to search for oviposition sites such as *D. wrightii* plants. Up to 200, light green to white eggs are deposited on the bottom of the plant's leaves, each measuring ~ 1.5 mm in diameter (Sasaki & Riddiford, 1984). One to eight days after oviposition the cylindrical, green colored larva emerges. *M. sexta*'s larvae can be distinguished from other hawkmoth species by their seven, diagonal white markings on the side of their bodies. Besides three pairs of thoracic legs, they have five pairs of prolegs. The larvae's terminal segment features a dorsal, dark red “horn”, which is eponymous next to their favorite host plant. In 21 days of development the larvae pass several larval stages and grow up to 6 cm. When the larvae reach their final larval stage, they stop eating, drop to the ground

and dig their way into the soil. Buried in the ground, pupae run through complete metamorphosis. Depending on temperature the pupation can take 19-21 days or even longer. At the end of the pupal stage the adult hawkmoths eclose and the life cycle starts all over again.

1.3 Morphology of *M. sexta*'s antennae

Antennae of adult *M. sexta* are highly structured, 2 cm long appendages of their heads, enabling the hawkmoths to detect a wide range of sensory stimuli such as gustation, olfaction and mechanoreception. As in other ectognathous insects *M. sexta*'s antennae can be divided into three different types of segments (Sanes & Hildebrand, 1976a). The two basal segments, proximal to the head capsule, are called scape and pedicel. Most proximal located is the scape, it links the antenna articulated to the insect's head and is the only antennal segment featuring muscles. Muscles of scape and head capsule allow for three-dimensional movements of the antenna. Attached to the scape and fixed to its musculature is the second, smaller segment, the pedicel. Into this segment a mechanoreceptive sensory system is incorporated, the Johnston's organ (Sanes & Hildebrand, 1976a). This chordotonal organ helps the insect to control its flight, sense air-currents and detect antennal vibrations for the perception of near-field sounds (Jarman, 2002; Yack, 2004). The third segment, the flagellum, is affiliated to the pedicle and is the antenna's most prominent feature, consisting of roughly 80, similarly shaped flagellomeres (aka annuli) (Keil, 1989; Sanes & Hildebrand, 1976a). Other than pedicel and scape, the flagellum is not directly linked to *M. sexta*'s musculature and can only be indirectly moved to the two basal segments. While the shape of flagellomeres from male *M. sexta* adults can be described as keyhole-like, cross-sections of female annuli are more or less round (Sanes and Hildebrand 1976a; Keil, 1989). This leads to the already mentioned sexual dimorphism of *M. sexta*'s antennae. In either case assembling of the many annuli, cause a tubular shape of the flagellum. This tube is filled with hemolymph from the insect's circulatory system, contains a trachea, a hemolymph vessel as well as two nerve bundles and is covered with a hard cuticle (Hildebrand & Sanes, 1976a). However the flagellum is still flexible due to more bendable cuticle at the intersegements between the individual annuli. The third segment hosts the major part of the antenna's sensilla, which are mainly located on the elongated side of each keyhole-like shaped annulus or on the medial

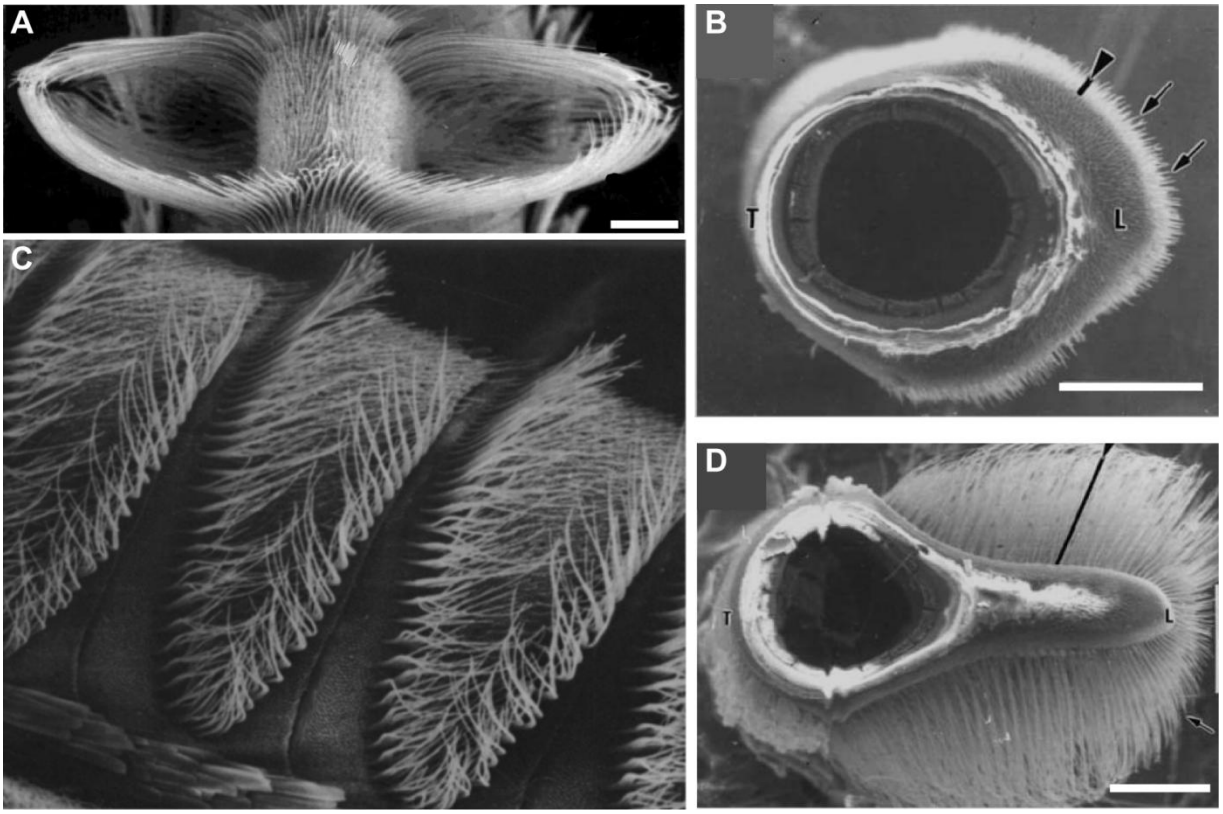

Fig. 1 | Antennae from female and male adult *Manduca sexta* differ in shape as well as in the presence of long setae which are called *sensilla trichoidae* and are limited to antennae of the male hawkmoth. (A-D) Scanning electron microscopy pictures of antennae from *M. sexta* adults. (A) Leading edge of a male hawkmoth's antenna. Trichoid sensilla type I form basket-like structures on annuli of the male antenna's flagellum. Scale bar 50 µm. (B, D) Cross sections of adult female (B) and male (D) flagella depict the sexual dimorphism of the hawkmoth's antennae. The females antennae exhibit a round shape, while antennae from male *M. sexta* adults are keyhole-like shaped. Prominent feature of the male's antenna are the long trichoid sensilla (D: black bar; modified from Shields & Hildebrand 1999a). Scale bar 250 µm. (C) Lateral view of the male antenna's flagellum. The trichoid sensilla are arranged in multiple rows and differ in length. Smaller setae are surrounded by longer sensilla. The trailing edge (bottom left) is covered with large scales. (Modified from Keil 1989)

hemi cylinder of female antennae. Annuli at the flagellum's base and tip are smaller than central located annuli, but due to fewer sensilla, their packing density remains the same. In both sexes, annuli are covered with scales opposite to the part bearing sensilla. This structure of the hawkmoth's antenna makes sure that during flight the sensilla can be directed forward (leading edge), while the scale covered parts point backwards (trailing edge) (Hildebrand & Sanes, 1976a). Besides their shape, female and male annuli differ in one more

striking feature (Fig. 1 B, D). The elongated side of male annuli bears multiple rows of long setae organized in U-shaped, basket-like structures (Fig. 1 A, C; Keil, 1989). This type of setae is referred to as *sensilla trichoideae* and are limited to male antennae. Only annuli at the flagellum's tip and base do not display these baskets composed of sensilla. Aside from the *sensilla trichoideae*, the antenna's flagellum bears also three other types of chemosensory sensilla: *sensilla trichoideae* type II, *sensilla basiconica, sensilla chaetica* and *sensilla coeloconica* (Altner & Prillinger, 1980; Keil & Steinbrecht, 1984; Lee & Strausfeld, 1990; Stengl et al., 1990). These sensilla are incorporated into the baskets or recessed in the flagellum's cuticle.

1.4 Morphology and anatomy of sensilla trichoideae type I

Trichoid sensilla type I cover male antenna's annuli in great numbers (~ 43000 per flagellum) and are irregularly perforated to enable an exchange of matter between their lumen and circumambient air (Fig. 2; Sanes & Hildebrand, 1976b; Keil, 1989; Lee & Strausfeld, 1990). The elongated seta is filled with sensillum lymph and houses two, unbranched dendrites of sensory neurons, which enable the insects to perceive pheromone components in their environment (Sanes & Hildebrand, 1976b; Keil, 1989). Each dendrite emanated from the apical pole of its respective sensory neuron's soma and is subdivided into an dendrite-sheath wrapped inner as well as an naked outer segment (Sanes & Hildebrand, 1976b; Keil, 1989). Extending into the sensilla's shaft, the cilia-like, outer dendrite lacks the central microtubule pair in its transition zone and neither possesses an endoplasmic reticulum nor any other cellular organelles (Keil, 1993). The two cell bodies of the bipolar sensory neurons lie directly underneath the cuticular channel of the trichoid sensilla. Originating from the neuron's soma and covered with a glia-sheath, two axons grow into the lumen of the antenna, join the antennal nerve and project into various glomeruli in the brain's antennal lobe. The odor- or pheromone sensitive sensory neurons are referred to as odorant receptor neurons (ORNs). From the two ORNs embedded in pheromone sensitive trichoid sensilla type I, one is responding to the pheromone blend's main component, bombykal (BAL: E10, Z12 hexadecadienal) (Dolzer, 2003). Besides BAL the female's pheromone blend contains eleven more volatile substances such as E10, E12-16:Al (EE); E10, E12, Z14-16:Al (EEZ); E10, E12, E14-16:Al (EEE) (Tumlinson et al., 1989). While eight of the blend's components are responsible for attracting male hawkmoths, already the two elements BAL and EEZ are

sufficient to trigger the males' mating behavior. Apart from the sensilla's BAL sensitive ORN, the second neuron is tuned to either EEZ, EE or EEE.

Along with the trichoid sensilla's two sensory neurons, three types of non-neuronal, glia-like sheath cells are embedded underneath this elongated setae: the thecogen cell, trichogen cell and tormogen cell (Sanes & Hildebrand, 1976b; Keil, 1989). The thecogen cell forms cell junctions like desmosomes and tight junctions with facing cell membranes, creating powerful barriers to prevent an exchange of ions as well as molecules between sensillum lymph and hemolymph. The trichogen cell partly envelopes the thecogen cell, anchored by close cell junctions. During the insect's development the trichogen cell secretes chitin to form the cuticulary shaft of the trichoid sensilla (Sanes & Hildebrand, 1976b; Keil, 1989). The trichogen cell's distal parts are wrapped by a third sheath cell: The tormogen cell lines the inner surface of the antrum almost up to the seta's shaft . Together with the trichogen cell it forms folds and microvilli at their apical membrane and creates a cavity for the sensillum lymph. Secreted by the trichogen and tormogen cell, the sensillum lymph exhibits an exceedingly high concentration (200 mM) of potassium-ions (Kaissling & Thorsen, 1980; Thurm & Küppers, 1980; Kaissling, 2009). This is achieved by V-ATPases generating a

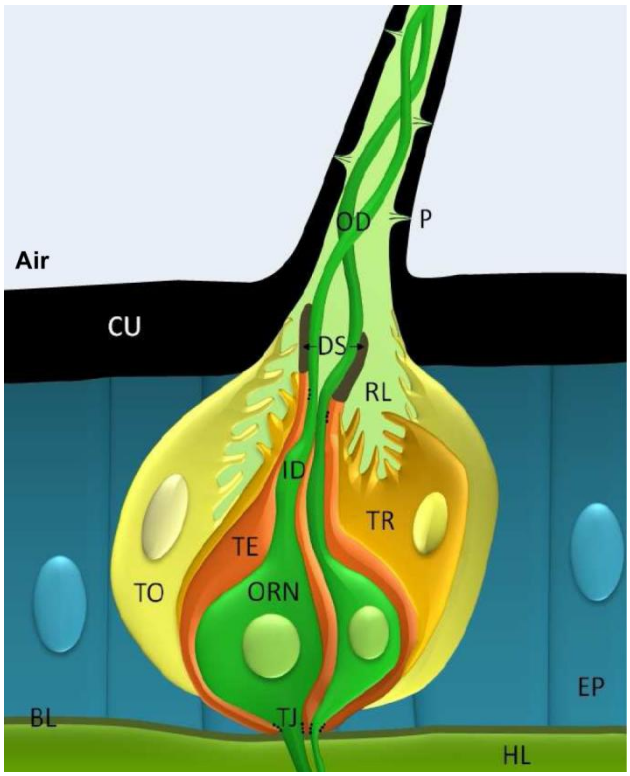

Fig. 2 | Schematic reconstruction of a trichoid sensillum type I from male *M.sexta* adults. Each *sensillum trichoideae* hosts two olfactory receptor neurons (ORNs). The ORNs unbranched dendrites project into the sensillum's shaft and are organized into an inner (ID) and an outer segment (OD). Two glia-like sheath cells, the tormogen (TO) and trichogen cell (TR) secrete chitin to form the sensillum's cuticulary shaft and produce the sensillum receptor lymph (RL). Cell protrusions from a third non-neuronal sheath cell (thecogen cell, TE) merge with the dendrite's sheath (DS) and due to tight junctions (TJ; black dots) only the OD contacts the RL. An exchange of pheromone and odor molecules between circumambient air and the RL is enabled by various pores (P) in the sensillum's cuticle (CU). Epithelial cells (EP), basal lamina (BL), hemolymph (HL); modified from Stengl 2010.

hydrogen ion gradient between sensillum lymph and cytoplasm (Wieczorek et al., 1991, 2003). Along with the H^+-gradient K^+/H^+-antiporters transport hydrogen ions into these cells while K^+-ions are translocated into the sensillum lymph's cavity (Wieczorek et al., 1991, 2003). Pumping cations into the sensillum lymph builds up a voltage-gradient along the ORNs, thereby supporting the generation of receptor potentials in the primary sensory neurons.

1.5 From perireceptor events to signal transduction

1.5.1 Odorant or pheromone molecules need help of transporter proteins to reach their point of final destination

Pore tubules in the cuticle of sensilla trichoideae type I or sensilla like sensilla basiconica enable passive diffusion of pheromone components or other odor molecules from circumambient air into the sensilla's cavity (Keil 1989). There the compounds are exposed to the hydrophilic sensillum lymph. In order to cross this fluid and to reach receptors incorporated in the dendritic membranes of the sensillum's ORNs, hydrophobic molecules like the pheromone's components have to bind to water-soluble transporter proteins. Depending on the bound molecule, these proteins are referred to as pheromone-binding proteins (PBP) or odorant-binding proteins (OBP), respectively (Leal et al., 2005 a, b). Both protein families are produced and secreted into the sensillum lymph by the sensillum's supporting cells. Compounds associated with PBPs or OBPs are not only transported across the aqueous sensillum lymph towards receptor proteins but are also protected from rapid degradation (Fig. 3; Kaissling, 2009).

Inactivation and degradation events in the sensillum lymph cavity have crucial effects on sensory adaptation and sensitivity as well as on the termination of the neuron's responses to an odor (Wybcrynski et al., 1989). The concentration of odorants in the sensillum lymph can be controlled by internalization in which the molecules are engulfed by the ORNs or by the non-neuronal sheath cells (Wybcrynski et al., 1989). Furthermore, enzymes may modify the

compounds' configuration to alternative conformations which are less active or even inactive (Wybcrynski et al., 1989). For instance, BAL as the main component of *M. sexta*'s pheromone blend, is oxidized by an aldehyde oxidase (AOX), expressed solely in antennal tissue (Wybcrynski et al., 1989).

1.5.2 The role of sensory neuron membrane proteins in the perception of odors or pheromones

After odorant molecules' binding to PBPs or OBPs, sensory neuron membrane proteins (SNMPs) may recognize and interact with these complexes, thereby translocating them proximately to the odorant's respective receptor (Benton et al., 2007). As their name already implies, SNMPs are located in the membrane of ORNs (Rogers et al, 1997, 2001 a, b; Benton et al., 2007; Forstner et al., 2008). Moreover they share homology to membrane located receptor proteins of the CD36 family, which are responsible for a controlled endocytosis of fatty acids, carotenoids and cholesterol esters (Rogers et al, 1997; Benton et al., 2007; Forstner et al., 2008). Besides SNMPs incorporated in the ORNs' membrane, it was possible to identify SNMPs which are located in the membrane of sheath

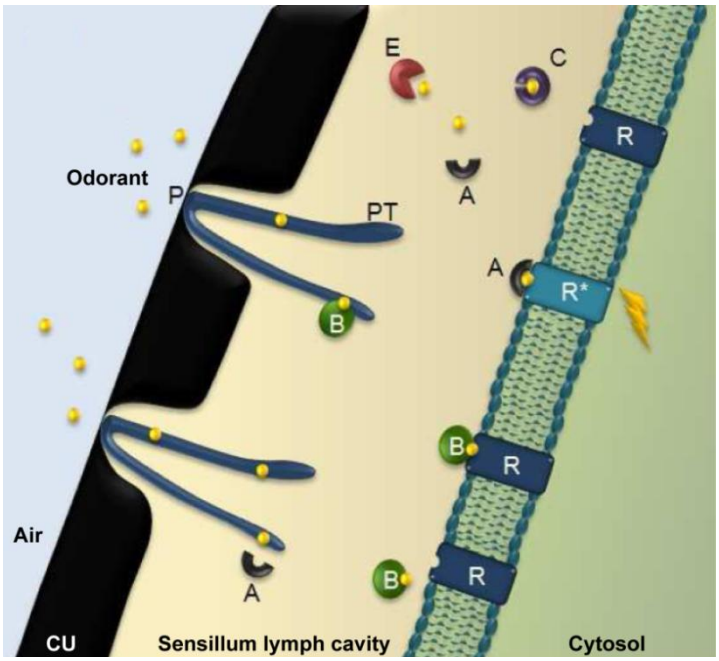

Fig. 3 | Schematic representation of perireceptor events in male *M. sexta*'s trichoid sensilla type I. Odor or pheromone components enter the sensillum via pores (P) and pore tubules (PT) in the shaft's cuticle. In order to cross the aqueous sensillum lymph, they bind to pheromone or odorant binding proteins (B). Escorted to their final destination the pheromone/odorant transporter complex interacts with their specific odorant receptor (R). This step not only activates the R (R*) and triggers a transduction cascade (bolt), but also leads to conformational change of the PBP/OBP to its A-form. A is released into the sensillum lymph. The pheromone/odorant is either enzymatically degraded (E) or kept from further binding events by its binding protein (C). (Modified from Nolte, 2010)

cells (Forstner et al., 2008). These SNMPs may contribute to the removal of lipophilic compounds (i.e. odorant molecules) from the sensillum lymph, controlling the odor concentration in the sensory organs cavity (Forstner et al., 2008).
Interaction of the SNMP-PBP/OBP-odorant complex with its specific receptor in the sensillum's dendritic membrane finally triggers a transduction cascade eventually leading to an odor response. At the same time, this binding step alters the transporter proteins current conformation, whereupon either the odorant or the SNMP-PBP-odorant complex is released into the sensillum lymph (Ziegelberger et al., 1990; Leal et al., 2005 a, b). In the sensillum's cavity the odor molecule is not only stopped from further interaction with its respective receptor but also enzymatically degraded (Wybcrynski et al., 1989).

1.5.3 Insect odorant receptor complexes

The ORN's odorant receptors (ORs) gated by the (SNMP)-PBP/OBP-odorant complex, form ion channels and belong to the 7 transmembrane (TM)- receptor protein superfamily (Clyne et al., 1999; Vosshall et al., 1999; Gao & Chess, 1999; Störtkuhl & Kettler, 2001; Hallem & Carlson, 2006;). Unlike many other members of this family the insect's ORs exhibit their C-terminus on the plasma membrane's extracellular side, while the N-terminus faces the cell cytoplasm (Benton et al., 2006; Wistrand et al., 2006; Hallem & Carlson, 2006; Lundin et al., 2007; Smart et al., 2008; Guo & Kim, 2010; Tsitoura et al., 2010). Thus the insect OR's membrane topology is inverted compared to vertebrate ORs. Whether or not an ORN is tuned to pheromone components or general odor molecules is governed by its expressed receptor subunits (Kaupp, 2010). Notable features of *M. sexta*'s ORNs are putative ultradian and circadian oscillations in subthreshold membrane potentials (Stengl, 2010). These spontaneous oscillations reduce or enhance the probability of reaching the neuron's action potential threshold (Larsson et al., 2004; Benton et al., 2007; Deng et al., 2011). For instance, superimposition of spontaneously elevated intracellular cation-levels and receptor potentials triggered by an odor or pheromone stimulus might exceed the threshold potential and eventually lead to an odor response. Thus, the depolarizing and hyperpolarizing phases of subthreshold membrane potential changes create a temporal preference for the perception of odors or pheromone (Stengl, 2010).
In *M. sexta* many key players involved in events before and upon binding of odor molecules to ORs have been scrutinized on gene and protein level, but only five different ORs have

been characterized so far (Große-Wilde et al., 2010). Amongst these ORs are two putative pheromone-specific odorant receptor proteins (MsexOR-1/4). According to previous findings from PCR-studies, MsexOR-1 and MsexOR-4 are solely expressed in male *M. sexta*-imagines (Große-Wilde et al., 2010). Transcription of both genes is restricted to different ORNs of the males' antennal trichoid sensilla (Große-Wilde et al., 2010). These ORNs are often adjacent to each other and their location matches with the location of pheromone-specific sensory neurons, suggesting that both ORs serve to detect two components of the hawkmoth's pheromone blend (Große-Wilde et al., 2010). Finally, besides a putative general odorant receptor (MsexOR-3), two ORs were identified which are only present in female adults (MsexOR-5/6). Comparative analysis of MsexOR-5 with related sequences in *Bombyx mori* led to the conclusion that this OR might be responsible for the detection of the plant odor linalool and therefore is involved in the following behavioral response (Große-Wilde et al., 2010).

1.5.4 The odorant receptor co-receptor eludes classification in serveral aspects

Consistent results from studies on higher insects indicate a co-expression of odor specific ORs with highly conserved membrane traversing proteins in an insect's ORNs (Krieger et al., 2002, 2003; Larsson et al., 2004; Couto et al., 2005; Goldman et al., 2005; Benton et al., 2006). These proteins are ubiquitous in olfactory organs of different insects (Hill et al., 2002a; Krieger et al., 2003; Pitts, Fox, & Zwiebel, 2004; Malpel et al., 2008; Patch et al., 2009) and were first identified in the model system *Drosophilia melanogaster,* where they were referred to as Or83b (Vosshall et al., 1999). In consequence of evidence for heteromerization of ORs and Or83b to a non-selective cation pore of unknown stoichiometry (Neuhaus et al., 2005; German et al., 2013), Or83b was renamed to DmelOrco (“odorant receptor co-receptor”) (Vosshall & Hansson, 2011). This nomenclature system refers to functional orthologs of DmelOrco across all insect species (e.g. MsexOrco or BmorOrco) (Vosshall & Hansson, 2011).

Co-expression of ORs and Orcos in heterologous expression systems provides evidence that both subunits contribute to the putative, OR-Orco ion channel's characteristics such as conductive properties or sensitivity to pharmaceuticals (Nichols et al., 2011; Pask et al., 2011; Nakagawa et al., 2012). Conflicting findings from tip recordings on *M. sexta* argue against an

involvement of MsexOrco in constituting odor-gated receptor complexes together with ORs (Nolte et al., 2013). Moreover, these results resemble observations from studies on Orcos from various insect species expressed in heterologous expression systems, where Orco was able to form homomeric ion-channels of unknown stoichiometry (Neuhaus et al., 2005; German et al., 2013). These pore complexes seem to be leaky cation-channels, sensitive to elevated intracellular cAMP/cGMP-levels and controlled by multiple phosphorylation events implemented via protein kinase C (Sato et al., 2008; Wicher et al., 2008; Jones et al., 2011; Sargsyan et al., 2011; Nolte et al., 2013).

Besides this controversial role of Orco, its function of mediating the localization of ORs to the outer dendritic membrane and its essential role in stabilizing OR complexes is well documented (Larsson et al., 2004; Benton et al., 2006). Due to the membrane localization and stabilization function of Orco which is crucial for odor detection, it is plausible that mutant fruitflies lacking the Orco gene cannot respond to odor stimulation anymore (Benton et al., 2006; Larsson et al., 2004; Neuhaus et al., 2005).

The recent synthesis and identification of allosteric drugs, directly activating or inhibiting Orco, finally represent an opportunity to make progress in the characterization of this key player in odor detection (Jones et al., 2011, 2012; Nichols et al., 2011; Pask et al., 2011, 2013; Bohbot & Dickens, 2012; Chen & Luetje, 2012; Taylor et al., 2012; Nolte et al., 2013; Röllecke et al., 2013). Just as lively debated as Orco's role in odor detection is the signal transduction following the binding of (SNMP)-PBP/OBP-odorant ligands to their specific OR complex.

1.6 Controversy in insect olfactory signal transduction

1.6.1 Pioneering work initiated reconsideration of mechanisms underlying olfactory signaling pathways

In 2008 conflicting publications pushed the research on transduction cascade events in insect olfaction forward. Sato et al. (2008) hypothesized that solely ionotropic mechanisms are responsible for triggering receptor potentials in response to odor or pheromone stimulation (Fig. 4 A). This model was based on findings from studies in which heterologously expressed OR/Orco complexes from various insect species induced very fast ionotropic responses, while the production of second messengers such as inositol-3-phosphate (IP_3), diacylglycerol

(DAG), cyclic adenosine monophosphate (cAMP) or cyclic guanosine monophosphate (cGMP) was depressed. Thus, Sato et al. concluded that signal transduction in ORNs is independent of G protein pathways. This suggestion is consistent with the fact that due to the insect ORs' inverted membrane topology, their C-terminus faces the membrane's extracellular side and therefore is not accessible for G proteins as a conventional binding domain (Nakagawa & Vosshall, 2009).

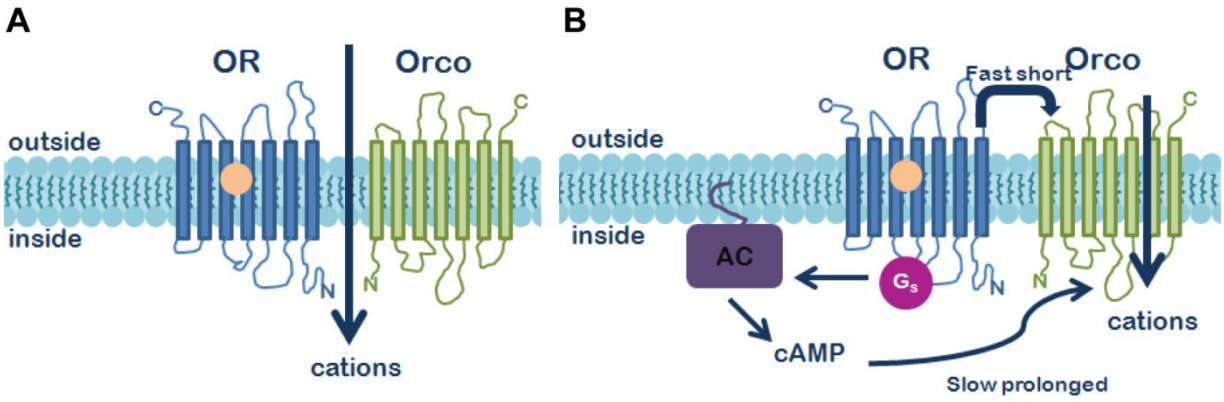

Fig. 4 | Controversial models of insect olfactory transduction. (A) The first model suggests that a variable odorant receptor (OR) unit and highly conserved olfactory receptor co-receptor (Orco) proteins form heteromeric non-selective cation channels. These ion channels are gated directly upon binding of odorant or pheromone molecules. Characteristics of triggered inward currents are independent of G protein pathways (Sato et al., 2008). (B) Wicher et al. (2008) hypothesized that the conventional ORs of the olfactory ion channel complex are coupled to trimeric G_s proteins while Orco subunits form additional cation channels. Characteristics of these Orco ion channels can be modulated directly or indirectly via intracellular cAMP and cGMP-levels. Odorant or pheromone binding to the OR-Orco channel complex not only induces a fast, short ionotropic inward current, but also leads to the release of $G_{s\alpha}$ units and subsequent activation of adenylyl cyclases (AC). AC-dependent production of cAMP entails a rise in internal cAMP-concentration which triggers a second, more sensitive and slower, metabotropic current. (Modified from Nakagawa & Vosshall, 2009)

Contrary to these results, Wicher et al. (2008) not only found evidence for a rapid, less sensitive, ionotropic response mediated by *Drosophila* OR22a/Orco, but also for a subsequent, slower, more sensitive, metabotropic cascade (Fig. 4 B). Thus, although there are no conventional binding domains for G proteins present in insect OR/Orco complexes, Wicher et al. (2008) detected an increase in intracellular cAMP-levels after initiation of the

metabotropic pathway. This phenomenon implies an evolution of yet unknown G proteins binding sites in the insect olfactory, 7 TM receptor complex.

Moreover, Wicher and colleagues observed heterologously expressed homomeric DmelOrco ion channels being gated by elevated cAMP/cGMP-levels and a decrease in the ion channels odor sensitivity when G protein signaling was inhibited. Based on these findings Wicher et al. (2008) presumed that the insect's olfactory metabotropic signal cascade activates adenylyl cyclases via $G\alpha_s$ proteins and serves as an amplification system enabling a perception of low odorant concentrations. Following studies could confirm stimulatory effects of elevated cAMP-concentration on the ORNs spiking rate (Deng et al., 2011; Olsson et al., 2011).

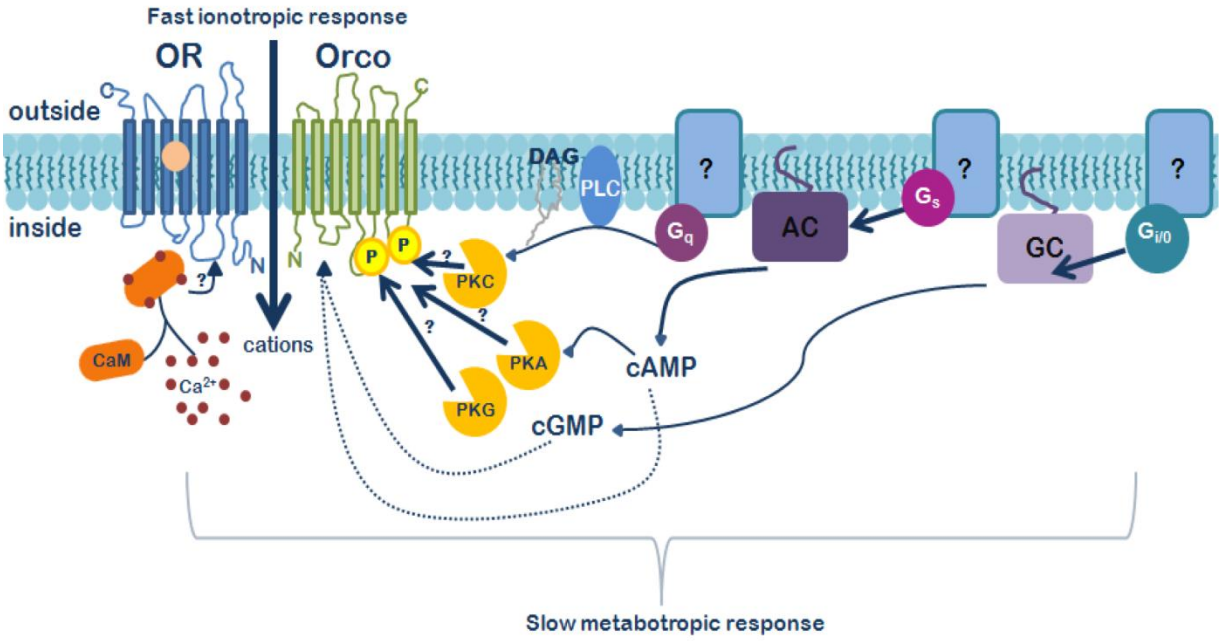

Fig. 5 | Model for an ionotropic odorant transduction pathway in insects which might be regulated metabotropically. In line with Sato et al. (2008) Vosshall and Nakagawa (2009) propose that odorant or pheromone-evoked cation currents are ionotropic and mediated by an odorant receptor (OR)- odorant receptor co-receptor (Orco) complex. Furthermore, Vosshall and Nakagawa (2009) note that elevated intracellular Ca^{2+}-levels could lead directly or indirectly via downstream effectors to alterations of characteristics of the OR-Orco ion channel's conductivity. Simultaneously, a co-activation of unidentified plasma membrane proteins could induce a production of multiple second messengers such as inositol triphosphate (IP_3), diacylglycerol (DAG), cGMP and cAMP. All metabotropic pathways together might contribute to tune the receptor more sensitive. (Modified from Nakagawa & Vosshall, 2009)

1.6.2 Model for ionotropic olfactory signaling cascades modulated by metabotropic events

Aspects from previously published models for insect odor transduction were combined in a "dual activation" hypothesis proposed by Nakagawa and Vosshall (2009; Fig. 5). This model assumes an initial, very fast ionotropic response upon ligand binding to an OR/Orco ion channel complex. Through the open pore formed by both, OR and Orco, cations enter the intracellular space, where the increased Ca^{2+}-levels indirectly (i.e. via calmodulin or via calmodulin dependend protein kinases) lead to modification processes of the already activated OR/Orco ion channel. Simultaneously either the elevated intracellular Ca^{2+}-concentration or an OR/Orco dependent co-activation of unidentified plasma membrane proteins trigger various downstream events such as the production of second messengers (IP_3, DAG, cAMP and cGMP). These molecules then change, together with Ca^{2+}-dependent effectors, the ion permeability of the activated OR/Orco ion channel, directly or via activation of protein kinases, tuning the receptor more sensitive.

1.6.3 Olfactory signal transduction could be realized via solely metabotropic processes

With her publication "pheromone transduction in moths" Stengl (2010) emphasized that it might not be possible to simplify insect signal transduction to one, generally valid mechanism. Furthermore she pointed out that different signal cascade pathways enable an insect to adjust its odor response in dependency on environmental influences, its physiological, metabolic as well as its behavioral status and on characteristics of perceived odor molecules. In contrast to the models mentioned above, Stengl monitored a metabotropic signal transduction cascade upon pheromone (BAL) stimulation in patch-clamp experiments on cultured primary ORNs from *M. sexta* antennae (Stengl et al., 1992; Stengl, 1993, 1994, 2010). Moreover, IP_3-treatment led to a sequence of three inward currents, similar to currents observed after application of BAL (Stengl et al., 1992; Stengl, 1993, 1994, 2010). Independent studies on the moth *Heliothis virescens* and other members of the phylum Arthropoda showed evaluated IP_3-levels in preparations of antennal tissue after application of species-specific pheromone and led to the discovery of rapid, transient rises in IP_3-concentration (Breer et al., 1990; Boekhoff et al., 1990; Boekhoff et al., 1993; Kaissling &

Boekhoff, 1993). These brief IP_3-signals returned rapidly to basal levels once they had

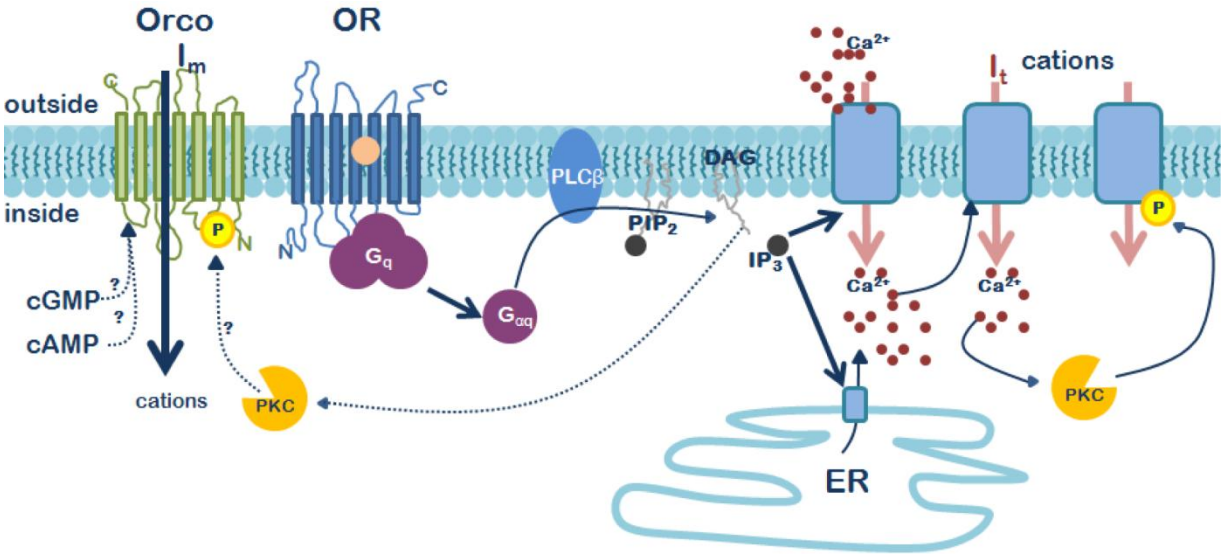

Fig. 6 | Schematic model of a soley metabotropic olfactory transduction in insects. Odorant or pheromone stimuli activate the G_q protein coupled olfactory receptor (OR) subunit of OR- olfactory receptor co-receptor (Orco) complexes. $G_{\alpha q}$ units are released and further activate phospholipase Cβs. Incorporated in the olfactory receptor neurons plasma membrane, PLCβ hydrolyzes phosphatidylinositol-4, 5-bisphosphate (PIP_2), producing inositol-triphosphate (IP_3) and diacylglycerol (DAG). Elevated intracellular IP_3-levels directly or indirectly gate Ca^{2+}-channels in the plasma membrane and endoplasmatic reticulum (ER) membrane. Further cation channel openings triggered by the rise in internal Ca^{2+}-concentration and phosphorylation events via protein kinase C (PKC) elicit further inward-, transduction currents (I_t). Moreover, activated by the increase in [Ca^{2+}] and [DAG], PKC might modulate the conformation of Orco subunits. This step might change the conductivity of Orco ion channels and their sensitivity to cyclic nucleotides. The solely metabotropic current (I_m) through Orco could eventually affect the ORNs spontaneous and background activity, modifying the neuron's response kinetics and shifting its dose-response curve (Getahun et al., 2013).

reached peak values about 50 ms after presentation of the stimulus (Breer et al., 1990; Boekhoff et al., 1990; Boekhoff et al., 1993; Kaissling & Boekhoff, 1993). Their occurrence within a millisecond time window resembled the timing of phasic odor-evoked action potential responses induced by short, millisecond-long exposure to physiological amounts of pheromone or odorants, respectively. Consistently, subsequent publications provided evidence for the presence of a PLCβ-subtype in pheromone sensitive moth ORNs (Laue & Steinbrecht, 1997; Maida, Redkozubov & Ziegelberger, 2000). Furthermore, their data

documented the existence of a G_q protein family possibly controlling the PLCβ activity and Ca^{2+}-ion channels gated by IP_3 (Laue & Steinbrecht, 1997). Hence, based on these facts, Stengl (2010, 2013) assumes that, mediated by BAL's binding to its receptor complex and the subsequent activation of $G_{q\alpha}$ units, PLCβ hydrolyzes its substrate phosphatidylionositol-4, 5-bisphosphate (PIP_2), producing the second messengers IP_3 and DAG. Then, IP_3-depending channel openings in the neuron's plasma membrane and the endoplasmic reticulum (ER) membrane could lead to an increase in internal, free Ca^{2+}-levels (I_t, Fig. 6). This rise in intracellular Ca^{2+}-concentration might trigger further [Ca^{2+}]-induced cation channel openings (I_t, Fig. 6). The high free, intracellular Ca^{2+}-levels together with phosphorylation events via activated PKCs could then gate a third class of ion channels, eventually leading to the ORNs depolarization (I_t, Fig. 6). However, neither the molecular identity of ion channel classes involved in the generation of the three pheromone-dependent inward currents, nor a possible role of Orco has been determined yet.

1.6.4 Is Orco involved in olfactory signal transduction mechanisms?

Current data from a study by Nolte et al. (2013) on *M. sexta* provides evidence against a (key) role of Orco in the generation of an OR/Orco mediated ionotropic signal cascade upon pheromone stimulation. Unexpectedly, *in vivo* perfusion of the Orco agonist VUAA1 into male hawkmoth antennae's trichoid sensilla failed to elicit an increase in receptor potentials or AP frequency during stimulation with BAL. Thus, the question remains whether there is any significance to the presence of Orco in the dendrites of *M. sexta'*s pheromone tuned ORNs, aside from membrane trafficking of ORs? In tip recordings Nolte et al. (2013) found evidence, that MsexOrco's activity influenced kinetics and sensitivity of pheromone responses within multiple seconds to minutes in a daytime dependent manner. Since Orco is quite likely capable of forming homomeric ion channels by itself which are not gated upon odorant or pheromone binding, these ion channels could define the ORN's intracellular, pre-stimulus cation levels. Oscillating depolarization of the neuron's membrane potential mediated by Orco would generate a temporal preference for the timing of stimulus inputs. Subsequently, elevated intracellular second messenger (Ca^{2+}, cGMP)-levels and PKC activity upon pheromone binding could then dose-dependently modulate the conductive properties of Orco ion channels (I_t, Fig. 6; Stengl & Funk, 2013). This would alter progress and sensitivity of elicited pheromone responses (Nolte et al., 2013; Stengl, 2010). Hence, second messenger-

sensitive Orco might be a key player in the generation of subthreshold membrane potential oscillations, controlling intracellular Ca^{2+}-levels and enabling mechanisms of temporal encoding. Most certainly, there is a need for further comparative studies on various insect species to resolve the events in signal transduction underlying insect odor/pheromone detection and to understand Orco's role in the sensory system of olfaction.

1.7 Calcium homeostasis

Most cells depend on strictly defined extra- and intracellular ion compositions maintained by their plasma membrane and its incorporated transport systems in order to survive. Even small changes in the inhomogeneous distribution of ions between the cell's inside and outside can have a tremendous impact on the physiological state of a cell. Thereby, the divalent-ions of the alkaline earth metal calcium take on an exceptionally important role. The disparity in extra- and intracellular concentrations of Ca^{2+} is particularly distinct, especially if compared to the distribution of other dietary nutrients like potassium, sodium and chlorine. Shifts in intracellular $[Ca^{2+}]_i$ are sufficient to control important cellular processes, such as gene transcription, cell proliferation and metabolism. Furthermore calcium-ions mediate cellular apoptosis by regulating mitochondrial function, movement and viability. They cross the mitochondrial outer membrane via diffusion and are translocated into the mitochondrial matrix by ion channels as well as transporter proteins (Clapham, 2007).

Besides that Ca^{2+} translates extracellular signals into internal responses. An increases in intracellular $[Ca^{2+}]_i$ can be accomplished either by changing the Ca^{2+}-fluxes through the plasma membrane or by releasing calcium-ions from internal pools (Simpson et al., 1995; Verkhratsky & Shmigol, 1996; Berridge, 1997). Calcium has various routes to enter a cell, amongst others through voltage-gated Ca^{2+}-channels as well as through store- or receptor-operated Ca^{2+}-channels (e.g. Verkhratsky & Shmigol, 1996; Parekh, 1997). Mechanisms elevating internal Ca^{2+}-concentrations over a certain threshold, tend to trigger Ca^{2+}-release from intracellular pools. Binding of phospholipase C generated IP_3 gates IP_3-receptors in the ER membrane. Aside from calcium-induced calcium-release, this step triggers Ca^{2+}-release from internal stores as well. Depletion of intracellular Ca^{2+}-pools induced either trough second messengers or calcium-ions, links extracellular with internal calcium-signaling (Parekh, 1997; Berridge, 1997; Putney, 2005): As a result of decreasing Ca^{2+}-levels in the ER, stromal

interaction molecule 1 (STIM1), an EF-hand protein incorporated in the ER membrane, merely encounters the divalent calcium-ion anymore (Srikanth & Gwack, 2012). The loss of STIM1's association with Ca^{2+} leads to the protein's oligomerization, followed by the oligomer's translocalization to ER plasma membrane junctions. In protein-protein interactions STIM1 facilitates clustering of Orai1 pores to store-operated Ca^{2+} (SOC) channels of the membrane (Srikanth & Gwack, 2012). Bound to STIM1 oligomers the Orai1 protein complexes increase their open probability, Ca^{2+} enters the cell and $[Ca^{2+}]_i$ raises. The elevated Ca^{2+}-levels do not only activate directly or indirectly a variety of downstream effectors but also exert negative feedback on the SOC channels. Non-excitable cells rely on Ca^{2+}-influx mediated by SOC-channels in order to raise their intracellular Ca^{2+}-concentration. Rises in free internal Ca^{2+}-levels are downregulated via cytosolic calcium-binding proteins and activity of Ca^{2+}-pumps in the plasma and ER membrane. These ATPases translocate calcium-ions across membranes either into the ER (sarcoendoplasmic reticular Ca^{2+}-ATPases; SERCA-pumps) or out of the cell (plasma membrane Ca^{2+}-ATPases; PMCA-pumps) (Clapham, 2007). Together with these PMCA-pumps Na^+/Ca^{2+} or Na^+/Ca^{2+}-K^+-exchanger control Ca^{2+}-extrusion.

1.8 Objective of the present study

As described above, function and key features of the ubiquitously in insect olfactory systems expressed co-receptor, involved in odor and pheromone transduction, are still objects of latest research and are under lively debate. To further characterize the sparsely understood Orco, we performed immunohistochemical studies as well as calcium imaging measurements on *M. sexta'*s heterologously expressed, ortholog of this protein, and *in situ* tip recordings on adult, male *M. sexta* antennae. Goals of this thesis were:

- Establishment of the recently identified Orco agonists OLC12 and VUAA4 as proper tools for MsexOrco's analysis *in situ* as well as in heterologous expression systems.
- Insight into dynamics as well as composition of Ca^{2+}-responses mediated by Orco oligomers heterologously expressed in CHO or HEK293 cell culture, respectively.
- Analysis of Orco activating or inactivating mechanisms.

Ion channels formed by Orco seem to have an essential role in an insect's olfactory system besides membrane trafficking of general odorant or pheromone-binding ORs. More knowledge about mechanisms underlying this key function together with availability of specific activators and blocker would greatly contribute to resolve unanswered questions in insect olfaction. Elucidation of events taking place in the sensory system of olfaction would not only enrich basic research but also help to develop insect repellents for pest control and stemming of insect-borne diseases.

2 Material and Methods

2.1 Cell lines

2.1.1 HEK293 cells

To investigate characteristics of the *M. sexta* Orco-ortholog (MsexOrco), Human Embryonic Kidney 293 (HEK293) cells stably transfected with MsexOrco were used. Transfection was performed by the company Cytobox located in Konstanz, Germany. Initially HEK293 cells derived from fetal kidney cells transformed with the adenovirus type 5. Latest findings provide evidence that HEK293 cells might descent from immature neurons (Shaw et al., 2002).

2.1.2 CHO cells

CHO cells were initially obtained by preparations of Chinese hamster ovaries and are popular heterologous expression systems for recombinant proteins. In order to compare findings for properties of MsexOrco with characteristics of DmelOrco, experiments were performed on Chinese hamster ovary (CHO) cells stably transfected with the *D. melanogaster* orthologue of Orco. Transfection, followed by fluorescence activated cell sorting (FACS), were conducted by Cytobox (Konstanz, Germany). The performance of FACS led to cell cultures with high expression levels of DmelOrco.

2.2 Cell cultures

HEK293 and CHO cell cultures were stably transfected with MsexOrco or DmelOrco. Cells were maintained at 37 °C, 100 % humidity as well as 5 % CO_2 and cultured in CYTOBOX^{TM} HEK select or CYTOBOX^{TM} CHO select medium, respectively. The culture medium was sourced from Cytobox and contained antibiotics as well as fetal calf serum (FCS) amongst

others. Included antibiotics favored selection of transfected and therefore resistant HEK293 and CHO cells. Transfected cells were incubated in coated standard culture flasks and grew to a confluence of 90 % before they were separated into new flasks every 2-3 days. Thus, a stop in cell growth caused by confluence was obviated. In order to transfer the cells into new culture flasks, the entire medium was removed and the inner surface of the flasks was rinsed with Ca^{2+} and Mg^{2+} free Hank's Balanced Salt Solution (HBSS).

Then 4.5 mL HBSS containing 0.5 mL trypsin were applied to the cell cultures and the flasks were swiveled so that adherent cells were resuspended and isolated from each other. After 2 min of incubation at room temperature (RT), enzymatic activity of trypsin was stopped by adding 5 mL of CYTOBOX™ HEK select or CYTOBOX™ CHO select medium plus FCS to the cells. The obtained cell suspension was transferred into 50 mL reaction tubes and centrifuged at 23.6 g (500 rpm) and RT for 4 min. Subsequently the supernatant was discarded and the residual cell pellet was re-suspended in CYTOBOX™ HEK select or CYTOBOX™ CHO select, respectively. Thereupon the cell count was determined and cells were passaged into new culture flask at a seeding density of $2.5 \cdot 10^4$.

2.3 Confocal laser scanning microscopy

In the 1950's Marvin Minsky developed the basic principle of confocal microscopy. In the following decades this method was further enhanced to today's confocal laser scanning microscopy (CLSM). In contrast to conventional wide-field techniques current CLSM allows deep-field micrographs while out of focus signals are not detected. In relation to improvements in optical resolution CLSM offers only small advantages over the wide-field technology. Though when combined with the use of fluorescent dye, CLSM is still a very popular method for providing high quality images, minimizing background information and producing thin optical sections.

Inserted specimens are punctiformly scanned with a coherent laser beam emitted by the microscope's incorporated multiple laser excitation source. On its way to the specimen the emitted light passes a first pinhole which is arranged confocal to a scanning point on the slide and focuses the beam even more. When the laser beam strikes the following dichromatic mirror, only light of previously defined wavelength is reflected, passes the objective and reaches the specimen. There, fluorophores are excited from a ground state to a state of

higher energy. This phenomenon is referred to as luminescence. While returning to the ground state absorbed energy (or parts of absorbed energy) is emitted in form of light emission. Due to its specific wavelength, secondary fluorescence generated by the fluorophores is now capable of passing the beam splitter instead of being reflected like the excitatory laser beam. The second pinhole filters out all signals which are not confocal with the pinhole and therefore out of focus. Finally, confocal secondary fluorescence hits the photomultiplier detector. Here a virtual, point by point reconstruction of incoming signals to a digital micrograph takes place. Hence the real image cannot be observed through the microscope's eye piece. However a great benefit of CLSM is the availability of a multi-channel detection mode where fluorochrome-signals with different or overlapping emission spectra can be captured simultaneously or sequentially.

2.4 Immunohistochemistry

HEK293 cells stably transfected with MsexOrco were transferred to poly-L-lysine coated glass cover slips and cultured at 37 °C, 100 % humidity and 5 % CO_2 in 24-well Plates. In a first step cells were fixed in PBS (in mM: KCl, 2.6; KH_2PO_4, 1.7; NaCl, 136; Na_2HPO_4, 10.1) with 4 % formaldehyde for 2 min at RT. After washing three times for 5 min in HBSS, cell membranes were stained via ten-minute incubation with solutions of Texas Red conjugated wheat germ agglutinine (WGA). Then HEK293 cells were rinsed again three times for 5 min in HBSS, followed by 60-minute preincubation in PBS with 5 % normal goat serum (NGS). In that manner nonspecific binding sites were blocked. Thereupon, incubation with the primary antibody was carried out at RT overnight in PBS which contained 5 % NGS and anti-Orco antibody at a dilution of 1:1000. After three rinsing steps for 5 min in PBS, cells were incubated with the second antibody Alexa® Fluor 488 at RT for additional 60 min. For this, secondary antibodies were diluted 1:1000 in PBS with 5 % NGS and added to the preparations. In a final rinsing cycle with three five-minute repetitions in PBS cells were pruned of remaining components from earlier steps. Preserved specimens were mounted on labeled cover slips with Entellan® and stored protected from light at 4 °C.

2.5 Fluorescence $[Ca^{2+}]_i$ measurements

In calcium imaging studies free intracellular Ca^{2+}-concentration of HEK293- or CHO cells stably transfected with MsexOrco or DmelOrco was evaluated more closely on basis of the fluorescence ratio method. Here, Fura-2 acetoxymethyl esters was used as a calcium-ion indicator. Cells were plated on poly-L-lysine coated glass-cover slips and grew for 48 h at 37 °C, 100 % humidity and 5 % CO_2 in 24-well Plates. Prior to the recordings cells were preincubated 30 min at RT in 1 mL culture media containing 2 µM membrane permeable Fura-2 AM. After two subsequent rinsing steps an additional incubation in 3 mL standard external solution (SES; in mM: $CaCl_2$, 1; KCl, 5; HEPES, 10; $MgCl_2.6\ H_20$ 1; NaCl 135) for 30 min at RT took place. Thus, unspecific artifacts during the calcium imaging recordings were avoided, resulting from quenching effects between Fura-2 AM and components of the culture medium.

Fluorescence $[Ca^{2+}]_i$ measurements were performed through brief, sequentially excitations of the Ca^{2+}-sensitive Fura-2 AM dye for 100 ms at wavelengths of 340 nm and 380 nm. The excitatory light beam was generated by a monochromator and then controlled and focused by a linked epifluorescence condenser. Thereby, the illumination system was controlled by an imaging control unit. Light emitted by the fluorescence dye passed a dichromatic mirror and a 420 nm long-pass filter, before reaching the image-forming elements of the coupled microscope. Observations of the cells were conducted with a 40x water immersion objective, while fluorescence images (resolution 640 x 480 pixel) were taken every 5 s over a period of 300 s or 600 s with a cooled CCD camera run by TILLVision 4.0 software. Based on the intensity ratios intracellular Ca^{2+}-levels were calculated:

$$[Ca^{2+}]_i = K_d Q \frac{(R - R_{min})}{(R_{max} - R)} \tag{1.1}$$

In this equation (1.1) R represents the fluorescence intensity ratios $F_{\lambda1}/F_{\lambda2}$ and the indices min and max are ratios representative for the particular titration endpoints (R_{min}, R_{max}). Fluorescence of Ca^{2+}-bound or free Fura-2 AM can be detected at wavelengths of 340 nm (λ1) and 380 nm (λ2), thus these are the selected wavelengths for relating recorded ratios to a certain Ca^{2+}-concentration. Q represents the ratio of the lowest (F_{min}) and highest (F_{max}) fluorescence signals at 380 nm (λ2). The final important variable is K_d as the Ca^{2+}-dissociation constant of Fura-2 AM. To calibrate the Ca^{2+}-indicator preliminary to the actual recordings, values for F_{min}, F_{max}, R_{min}, R_{max} and K_d were ascertained. Therefor the ratios for

completely Ca^{2+}-free and saturated Fura-2 AM were determined as well as fluorescence signal ratios at a third defined, free Ca^{2+}-concentrations (Ca^{2+}-free, 5 mM Ca^{2+}, 500 nM Ca^{2+}; thereby composition of the latter solutions was computed using WINMAXC v.2.20), while cells were permeabilized with 2 µM ionomycin .

2.6 Drug treatment

To investigate whether the drugs OLC12 and VUAA4 (structure Fig. 11 B, C) serve as agonists of MsexOrco, 100 µL of the substances were applied to SES while monitoring the $[Ca^{2+}]_i$-levels (see chapter 2.5) of the transfected cells (HEK293). The compounds were dissolved in dimethyl sulfoxide (DMSO) and diluted to working solutions of 100 µM (OLC12)

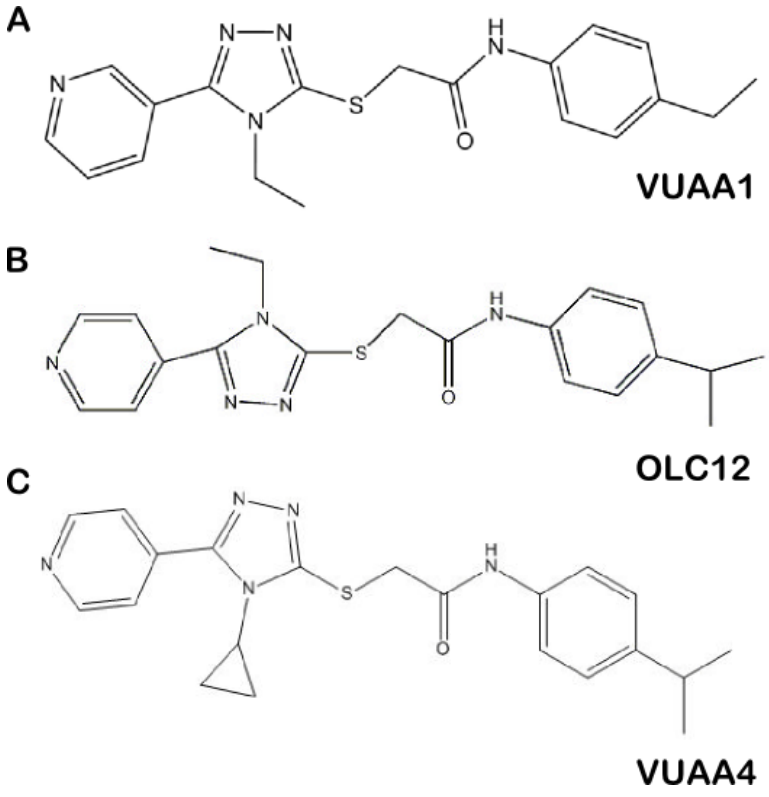

Fig. 7 | Chemical structure and abbreviations of the Orco agonists utilized in this thesis. OLC12 and VUAA4 originate from chemical modifications of the parent structure VUAA1 (2 - (4-ethyl-5 - (pyridine - 3 –yl) – 4 H-1, 2, 4– triazol– 3 -ythio)– N -(4 -ethylphenyl) acetamide). These agonistic drugs are thought to bind to a yet unidentified Orco intrinsic binding pocket and activate the Orco-formed ion channel (Jones et al., 2011, 2012; Chen & Luetje, 2012; Taylor et al., 2012).

and 10 µM (VUAA4) in SES. After 50 s of calcium imaging recording, the solutions were added via pipettes. Kinetics and amplitude of the triggered Ca^{2+}-responses were compared to responses of CHO cells stably transfected with DmelOrco. Therefor, we used the same stock solutions and working concentration of OLC12 and VUAA4 as described above.

Furthermore the involvement of internal Ca^{2+}-pools in the response of DmelOrco expressing CHO cells to activation via Orco antagonists was evaluated. First, a putative Ca^{2+} induced calcium release (CICR) from inner stores was inhibited. In calcium imaging recordings ryanodine was used, as a blocker of ryanodine receptors (RyR). Additional, dantrolene was employed to prevent intracellular Ca^{2+}-release. Cells were pretreated with 100 µL of 100 µM ryanodine respectively 10 µM dantrolene 25 s prior to applications of 100 µL OLC12 (100 µM). Next internal Ca^{2+}-pools were depleted by preincubating cells in SES containing 100 µM thapsigargin, which blocks the sarco-endoplasmic reticulum Ca^{2+}-ATPase, 40 min before calcium imaging experiments. To determine whether direct calcium-ion release from internal stores alters Orco mediated Ca^{2+}-signals, 100 µL of 20 mM caffeine as a RyR agonist, was added to the bath 75 s prior to OLC12 application.

Finally, elevated internal Ca^{2+}-levels close to the plasma membrane were mimicked, pretreating cells with 100 µL of 1 µM or 100 nM ionomycin 225 s before adding OLC12. As a representative of ionophore molecules, ionomycin transports calcium-ions across the lipid bilayer of a cell's plasma membrane and raises the intracellular Ca^{2+}-concentration.

Except for incubation of cells in SES containing thapsigargin, all drug treatments were performed during $[Ca^{2+}]_i$-measurements. Caffeine was dissolved in H_2O and diluted in SES. All other drugs were dissolved in DMSO and diluted to their working concentration in SES just like OLC12 and VUUA4.

2.7 Data analysis calcium imaging

Recorded fluorescence images were analyzed with TILLvision 4.0 software. Cells displaying changes in $[Ca^{2+}]_i$ during measurements were marked as Regions of interest (ROIs). To relate the recordings to certain Ca^{2+}-concentrations, the average fluorescence ratio of each ROI was calculated thereby subtracting the background fluorescence. The rate of the recorded decline in intracellular Ca^{2+}-levels is described by a first-order process:

$$[A] = [A]_0 \cdot e^{-k_1 t} \tag{1.2}$$

$$[A] = [A]_0 \cdot e^{\frac{-t}{\frac{1}{k_1}}} = [A]_0 \cdot e^{-t/\tau} \tag{1.3}$$

Where $[A]_0$ represents the initial concentration of product A, [A] is the concentration of A at a certain point of time (t) and k_1 stands for the rate constant. In order to analyze the kinetics of triggered Ca^{2+}-signals, the τ values for the falling phases of the different responses were calculated. First the rate constant k_1 for the decline in Ca^{2+}-levels was determined using PRISM 4, then τ ($1/k_1$) was assessed. Subsequently, the observed mean changes in intracellular Ca^{2+}-levels ($\Delta[Ca^{2+}]_i$) were evaluated by performing area under the curve (AUC) analysis of the particular signals in Microsoft Excel (2007). Evaluation focused only on the Ca^{2+}-profile's parts after application of control solutions or agonists. These regions of the curve were divided into series of trapezoids. After these areas were summed up, the results were divided by the number of trapezoids (n-1; 48), multiplied with the interval between to data points (t_{j+1}-t_j; 5 s; 1.4/1.5):

$$\overline{\Delta}[Ca^{2+}] = \frac{AUC}{(n-1)\cdot(t_{j+1}-t_j)} \tag{1.4}$$

$$AUC = \sum_{j=1}^{n-1} \frac{([Ca^{2+}]_i)_j + ([Ca^{2+}]_i)_{j+1}}{2\cdot(t_{j+1}-t_j)} \tag{1.5}$$

Statistical analysis was performed with PRISM 4. By using the normality test function (D'Agostino-Pearson omnibus test) of PRISM 4 it was tested if the data followed a normal distribution. In case of a normal distribution the student t-test (sample pairs) or One-Way-Anova (three or more groups) was utilized. Non-parametric data was compared using the Wilcoxon-Mann-Whitney test for sample pairs or Kruskal-Wallis test for three or more groups.

2.8 Tip recordings

In tip recordings it was validated whether or not VUAA1 and related substances applied into the hemolymph system of male *M. sexta* antennae can cross cell barriers of sheath as well as epidermis cells surrounding odorant receptor neurons and modulate the neurons' spontaneous activity patterns. Therefor, recordings were performed with hemolymph ringer solutions containing 100 µM or 1 mM VUUA1. Additional experiments were performed to

investigate if VUAA1 is capable of diffusing into trichoid sensilla of *M. sexta* through the sensilla's pores, thereby reaching the incorporated ORNs' dendrites and altering their spontaneous activity levels. Since VUAA1 and related compounds are not volatile, a pipette tip was put on the male moth's antennae. The pipette tip was backfilled with sensillum lymph ringer containing 100 µM VUAA1, fixed with dental wax and the proximal end was sealed with electrode gel. After 60 minutes of incubation, the actual tip recordings were performed. Prior to both tip recording trails male *M. sexta* adults were fixated in teflon holders. To prevent artifacts during the recordings due to movement of the antennae, the antennae's flagellum was immobilized with dental wax. All recordings were performed under supervision and guidance of Andreas Nolte. For the experiments, the antennae's first 15 apically located annuli needed to be truncated in order to insert a sharpened glass-capillary electrode, used as an indifferent electrode. According to the addressed problem, the electrode was either filled with pure hemolymph ringer or with hemolymph ringer containing VUAA1. After the glass electrode's tip had been placed underneath sensilla of the second annuli, the antennae's distal end was sealed with electrode gel obviating its dehydration. To establish an electrical contact between sensilla lymph and recording electrode, a sharpened glass-capillary electrode was filled with pure sensillum lymph ringer. Next, the upper parts (~1/4) of the secondary sensillum were cut off and the glass electrode was slipped over the sensillum using a micromanipulator. For positive controls, the sensillum lymph ringer contained 100 µM VUAA1.

Both electrodes were made of Ag/AgCl coated silver wires and were connected by ringer solutions. ORNs in the sensillum lymph shaft were recorded continuously for 295 s (Clampex 8) multiple times. Detected voltage changes between both electrodes (transepithelial potential) originating from the neurons' spontaneous, pheromone-independent generation of action potentials (APs), were first amplified 200-fold by a high-impedance amplifier and then sampled at a rate of 20 kHz via Clampex 8 for each trigger event. Due to the fact that ORNs of trichoid sensilla produce APs of different amplitude, obtained data was assigned to two different neurons and only one data set was used for further analyses.

2.9 Ringer solutions

All glass electrodes for tip recordings were filled either with hemolymph Ringer (in mM: $CaCl_2$, 1.0; D-glucose, 22.5; HEPES, 10.0; KCl, 171.9; $MgCl_2$, 3.0; NaCl, 25.0) or sensillum lymph

Ringer (in mM: $CaCl_2$, 1.0; D-glucose, 354.0; HEPES, 10.0; KCl, 171.9; $MgCl_2$, 12.0; NaCl, 12.0) in order to establish contacts between electrodes and the insect's relative circulatory system. To mimic the hemolymph's and sensillum lymph's osmotic state as well as the pH value, first the solutions' pH was adjusted to 6.5. Next mannitol was added to the Ringer solutions till they reached an osmolarity of 450 mOsmol/L (hemolymph Ringer) or 475 mOsmol/L (sensillum lymph Ringer). Stock solutions of VUAA1 dissolved in DMSO were diluted to working solutions of 100 µM and 1 mM in hemolymph ringer. Furthermore, VUAA1 stock solutions were diluted to a concentration of 100 µM in sensillum lymph ringer. All VUAA1 working solutions contained 0.1 % DMSO and were stored at -20 °C.

2.10 Animal rearing

Tip recording experiments were performed on one to two day(s) old, adult males of *M. sexta*, taken from populations of the Department of Animal Physiology, University Kassel. Moths of both sexes were kept together in one fly chamber. They were allowed to feed on sugar solutions *ad libitum* and flight cages contained *Nicotiana attenuata* plants for oviposition. Three times a week eggs were gathered from the plants into small plastic boxes. From the first day after hatching, larvae fed on an artificial diet (ingredients for 4 kg: 85 g agar, 1155 g wheat flour, 1155 g rye flour, 1250 g soy flour, 308 g casein, 11.6 g NaCl, 11.6 g calcium carbonate, 116 g ascorbic acid, 38.5 g sorbic acid, 38.5 g methyl paraben, 4.5 ml linseed oil, 30 mg nicotinic acid, 15 mg riboflavin, 7 mg thiamin, 7 mg pyridoxine, 7 mg folic acid and 0.6 mg biotin per 1.8 ml water) and were transferred regularly into clean, bigger boxes. As soon as larvae reached the wandering state (three to four weeks) they were isolated and placed into pupation chambers drilled into lumbers. There the larvae stayed for pupation (~ three weeks) until three days before the putative hatching date. These pupae were sorted by sex and then selected for experiments or further rearing. For tip recordings male pupae were rinsed with 70 % ethanol and reared separately from females to prevent uncontrolled exposure to sex pheromone. All animals, from larvae to imagines, were kept under long-day conditions (Light:Dark= 17 h:7 h) at 24-27 °C and 40-60 % humidity.

2.11 General Chemicals

The phosphate buffered saline (PBS) utilized for immunohistochemistry contained potassium and sodium chloride sourced from Roth (Karlsruhe, Germany) as well as disodium hydrogen phosphate plus monopotassium phosphate delivered from Sigma Aldrich (Taufkirchen, Germany). Magnesium chloride, potassium chloride, sodium chloride, sodium hydroxide as ingredients of the standard external solution (SES) used in calcium imaging recordings were procured from Roth. The buffer's remaining components calcium chloride, D-(+)-glucose and HEPES were produced by Sigma Aldrich. Sodium hydroxide and hydrogen hydroxide obtained from Sigma Aldrich, were used for adjusting the pH-value of all listed buffer solutions.

Rye, soy and wheat flour for the artificial diet of *M. sexta* larvae was delivered from Adler Mühle located in Bahlingen, Germany. All other solid components of the larvae's food were purchased either from Roth like agar-agar, ascorbic acid, biotin, folic acid, nicotinic acid, pyridoxine, riboflavin, sodium chloride, sorbic acid as well as thiamin or from Sigma Aldrich like calcium carbonate, casein and methyl paraben. Linseed oil was produced by Frisan (Nürnberg, Germany) and sugar for the artificial nectar for feeding the imagines was obtained from Roth. Aside from mannitol which was sourced from Roth all other chemicals contained in the hemolymph and sensillum lymph ringer were already present, their origin is described above (see PBS-buffer and SES).

2.12 Special chemicals

To maintain cell cultures the media CYTOBOX™ HEK select or CYTOBOX™ CHO select were purchased by Cytobox. Furthermore EDTA was sourced from Sigma Aldrich; FCS from PAA (Pasching, Austria) and trypsin from Sigma Aldrich. Immunohistochemistry was performed using Alexa fluor® goat anti-rabbit IgG obtained from Invitrogen (Carlsbad, USA); Entellan® from Merck (Darmstadt, Germany); formaldehyde and poly-L-lysine from Sigma Aldrich. HBSS as well as normal goat serum were sourced from Invitrogen. The MsexOrco antibody was kindly provided by Jürgen Krieger (Hohenheim, Germany). Fluorescence dye utilized in calcium imaging recordings was sourced from Invitrogen. For pharmacological characterization of monitored cells caffeine, dantrolene, ionomycin, ryanodine and

thapsigargin were delivered from Sigma Aldrich. VUAA1 and its related substances OLC12 as well as VUAA4 were synthesized by the working group “Mass Spectrometry/Proteomics” Max-Planck Institute for chemical ecology (Jena, Germany). All water-insoluble chemicals were dissolved in DMSO obtained from Sigma Aldrich.

2.13 Material

Name	Producer
Petri dishes	Greiner Bio-One (Solingen, Germany)
Culture flasks	Sarstedt AG (Nürnbrecht, Germany)
24-well Multiwell-plates	Sarstedt AG (Nürnbrecht, Germany)
Round cover slips	Roth (Taufkirchen, Germany)
Glass-capillary	Harvard Apparatus (Edenbridge, UK)

2.14 Equipment

Device	Producer
Incubator HERAcell 150	Heraeus Instruments (Hanau, Germany)
Fluorescence microscope Axioscop	Carl-Zeiss (Oberhausen, Germany)
Vortex Shaker, VortexGenie 2	SI – Scientific Industries (NY, USA)
pH-Meter 766 Calimetric	Knick (Berlin, Germany)
LSM 501 Meta	Carl-Zeiss (Oberhausen, Germany)
Incubator C42	Labotect (Göttingen, Germany)
ME 23 AP analytic scale	Sartorius AG (Jena, Germany)
Polychrome V	TILL Photonics (München, Germany)
Polychromator Imaging control unit	TILL Photonics (München, Germany)
Universal 320 centrifuge	Hettich (Tuttlingen, Germany)
Micromanipulator tip recordings	Leitz (Wetzlar, Germany)

2.15 Software

Name	Producer
Adobe® Illustrator® CS6	Adobe systems (München, Germany)
Adobe® Photoshop® CS6	Adobe systems (München, Germany)
GraphPad PRISM® Version 4.0	GraphPad (La Jolla, USA)
MSOffice 2007	Microsoft Cooperation (Redmond, USA)
TILLVision Version 4.0	TILL Photonics (München, Germany)

3 Results

Function and activity of tuning ORs is impaired in absence of the highly conserved Orco (Larsson et al., 2004; Neuhaus et al., 2005; Taylor et al., 2012), whereas sole expression of Orco monomers leads to formation of functional, homomeric cation channels (Wicher et al., 2008; Stengl, 2010; Jones et al., 2011; Nolte et al., 2013). These ion channels of unknown stoichiometry cannot be gated by odorants or pheromones but are activated upon binding of allosteric ligands (Jones et al., 2011; Taylor et al., 2012; Nolte et al., 2013). To learn more about properties of these Orco oligomers, independent of putative other ion channels involved in insect olfaction, MsexOrco was heterologously expressed without conventional ORs in human embryonic kidney (HEK293) cells. This common expression system has proven itself helpful in previously studies on characteristics and function of ORs and Orco orthologs from different insect species. Preliminary to further examination of MsexOrco's key features, the co-receptor's distribution and level of membrane association in the stably transfected cell line was evaluated.

3.1 Distribution of MsexOrco in HEK293 cell cultures

Initially the protein’s expression level was quantified via immunochemistry (Fig. 8). Confocal laser images were obtained by executing multi-track scans at 488 nm and 542 nm wavelength. Monitored cells did show fluorescence signals for Orco-epitopes (~ 10 %, Fig. 9). However the majority (~ 90 %, Fig. 9) of cells did not display Orco-like immunoreactivity, indicating weak expression levels of MsexOrco.

For additional information about the Orco’s degree of plasma membrane association, membrane staining was performed. Colocalization of immuno- and membrane staining was detected in ~ 2 % (Fig. 8 B-E; Fig. 9) of analyzed HEK293 cells (n= 304). Comparison of these fluorescence signals indicated a sparse membrane association of MsexOrco (Fig. 8 B-E; Fig. 9). Furthermore the intensity profile of most Orco-immunoreactive cells alluded a predominate, cytoplasmic localization of Orco (Fig. 8 B-E). Controls without first or second antibody as well as controls missing WGA ruled out autofluorescence of the expression system and significant, unspecific effects of the used antibody.

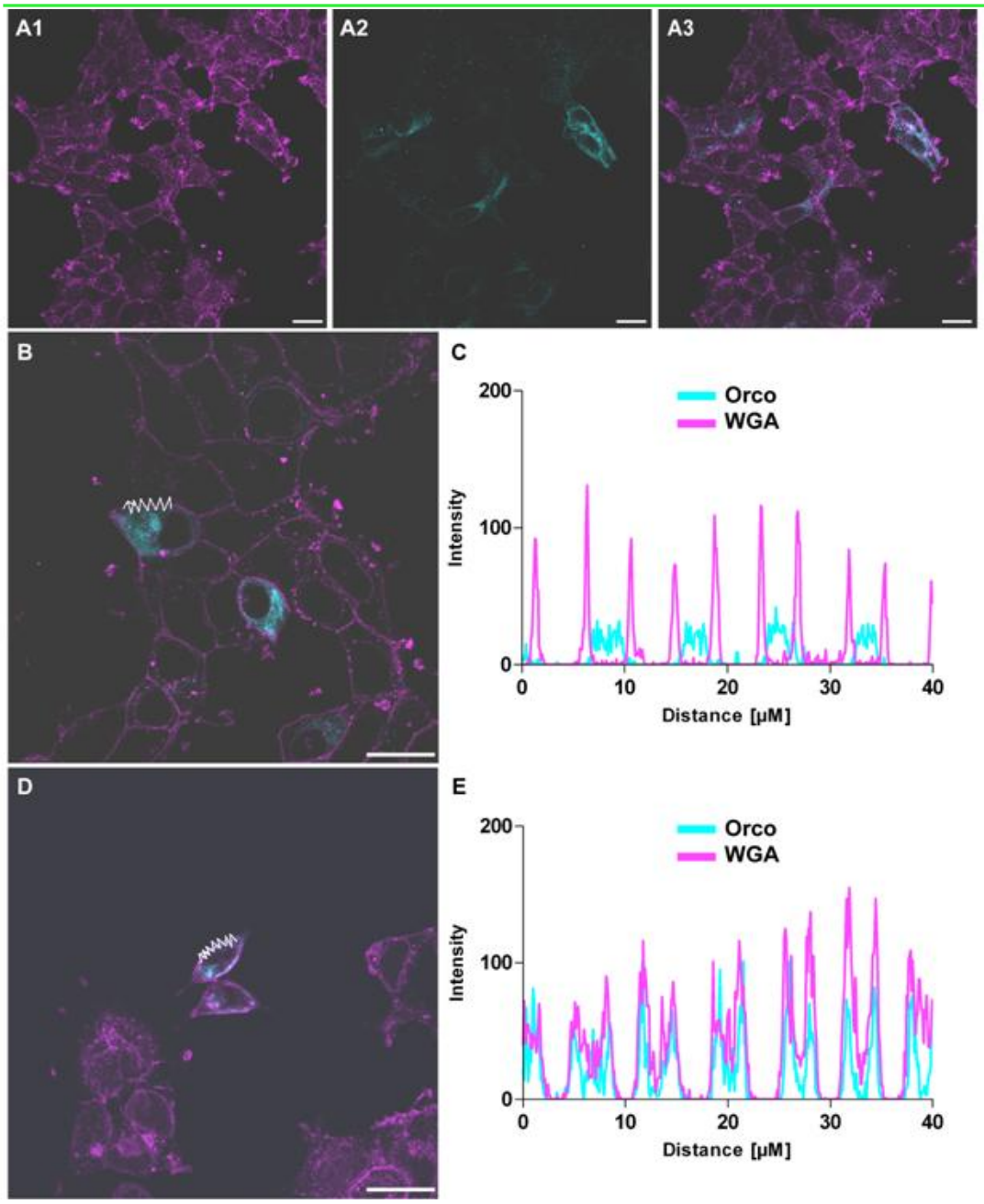

Fig. 8 | HEK293 cells stably transfected with MsexOrco showed weak fluorescence signals for Orco-epitopes, however the expression level was very low. Moreover, if MsexOrco was expressed, it was not necessarily associated with the plasma membrane. (A1-A3, B, D) Confocal laser scanning images of HEK293 cells stably transfected with MsexOrco. Cyan: immunofluorescence Orco; magenta: Texas-Red fluorescence of Wheat germ agglutinine (WGA) labeled plasma membranes. (B, D) MsexOrco expressing HEK293 cells picked for further analysis of putative plasma membrane association. White lines illustrate position and path length of intensity profiles in (C) and (E). Scale bar 20 µM. (C, E) Intensity profiles of MsexOrco immunofluorescence and WGA-membrane labeling. Overlap of both signals point to a plasma membrane association of MsexOrco.

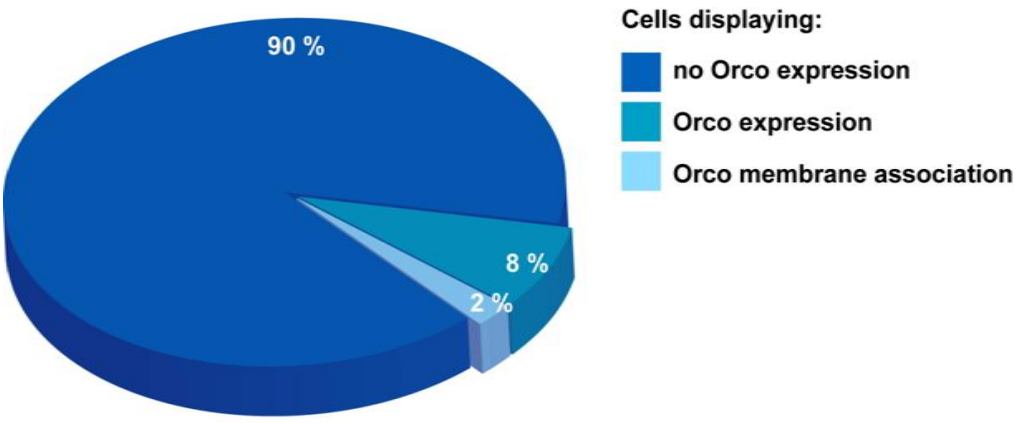

Fig. 9| The majority of monitored cells from HEK293 cultures stably transfected with MsexOrco did not express the co-receptor. Pie chart representing the percentage of surveyed cells (n= 304) showing Orco-like immunoreactivity. The level of plasma membrane association was analyzed via comparison of intensity profiles of Orco immunofluorescence signals and WGA-membrane labeling.

3.2 Effects of OLC12 and VUAA4 on MsexOrco transfected HEK293 cells

In the following calcium imaging experiments MsexOrco transfected HEK293 cells were exposed to 100 µM OLC12 or 10 µM VUAA4 over a period of 250 s (Fig. 10 A, C). Although most cells did not respond to the stimuli, a few showed an increase in intracellular Ca^{2+}-levels (Fig. 10, Fig. 13). Induced changes in mean intracellular Ca^{2+}-concentrations were relatively small, though highly significant compared to Ca^{2+}-signals in non-transfected HEK293 cells (OLC12: ****P < 0.0001, VUAA4: ****P < 0.0001; Fig. 13 A1-B2).

The responding HEK293 cells displayed direct reactions to the agonist's application in form of rapid rises in intracellular Ca^{2+}-concentrations, succeeded by falling phases with mean durations of ~ 66 s for OLC12 and ~ 115 s for VUAA4.

Results from additional recordings with non-transfected HEK293 cells proofed that Orco and no other ion channel is the drugs' specific target. OLC12 and VUAA4 failed to elicit any Ca^{2+}-signals in this empty expression system (Fig. 10 B, D). Taken together, the above findings confirmed that both OLC12 and VUAA4 serve as activators of MsexOrco. While both agents induced transient Ca^{2+}-signals, their magnitude varied. MsexOrco transfected cells responded to the presence of OLC12 with a distinct, lower mean increase in $[Ca^{2+}]_i$ compared to VUAA4 (Fig. 13 B). Since the compounds' applied concentrations differed, VUAA4 seems to have a higher potency than OLC12.

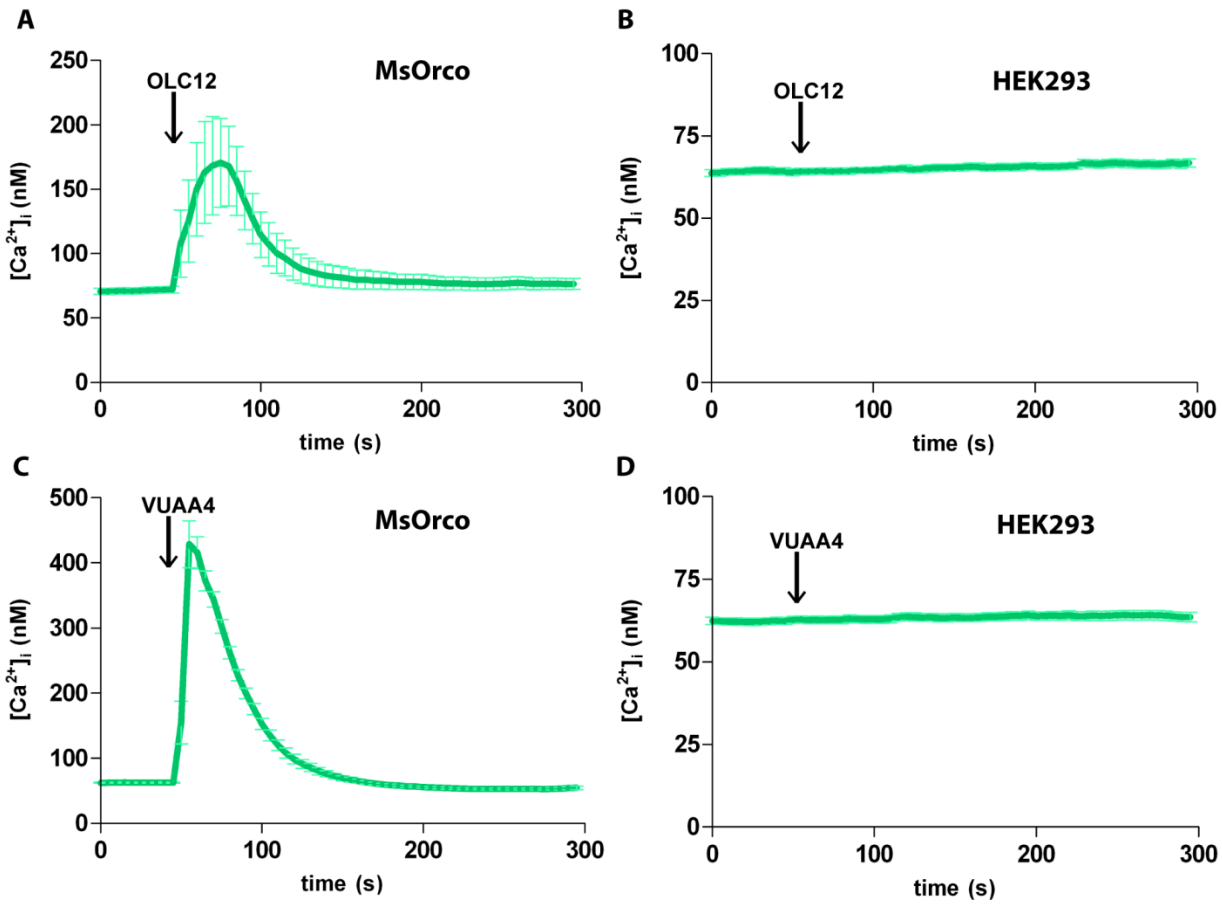

Fig. 10 | OLC12 and VUAA4 induced MsexOrco mediated Ca^{2+}-signals in a heterologous expression system. Kinetics and magnitude of triggered Ca^{2+}-response differed between both Orco agonists. Intracellular Ca^{2+}-levels of non-transfected HEK293 cells are not affected by the presence of OLC12 and VUAA4. Effects of 100 µM OLC12 or 10 µM VUAA4 on HEK293 cells stably transfected with MsexOrco (A, C) or on non-transfected HEK293 cells (B, D). Each graph represents the mean values for the different recordings gained by averaging the Ca^{2+}-concentrations of all signals at each time point. Compounds were applied after 50 s of recording. Analyzed cells: (A) n=11, (B) n=50, (C) n=49 and (D) n=52.

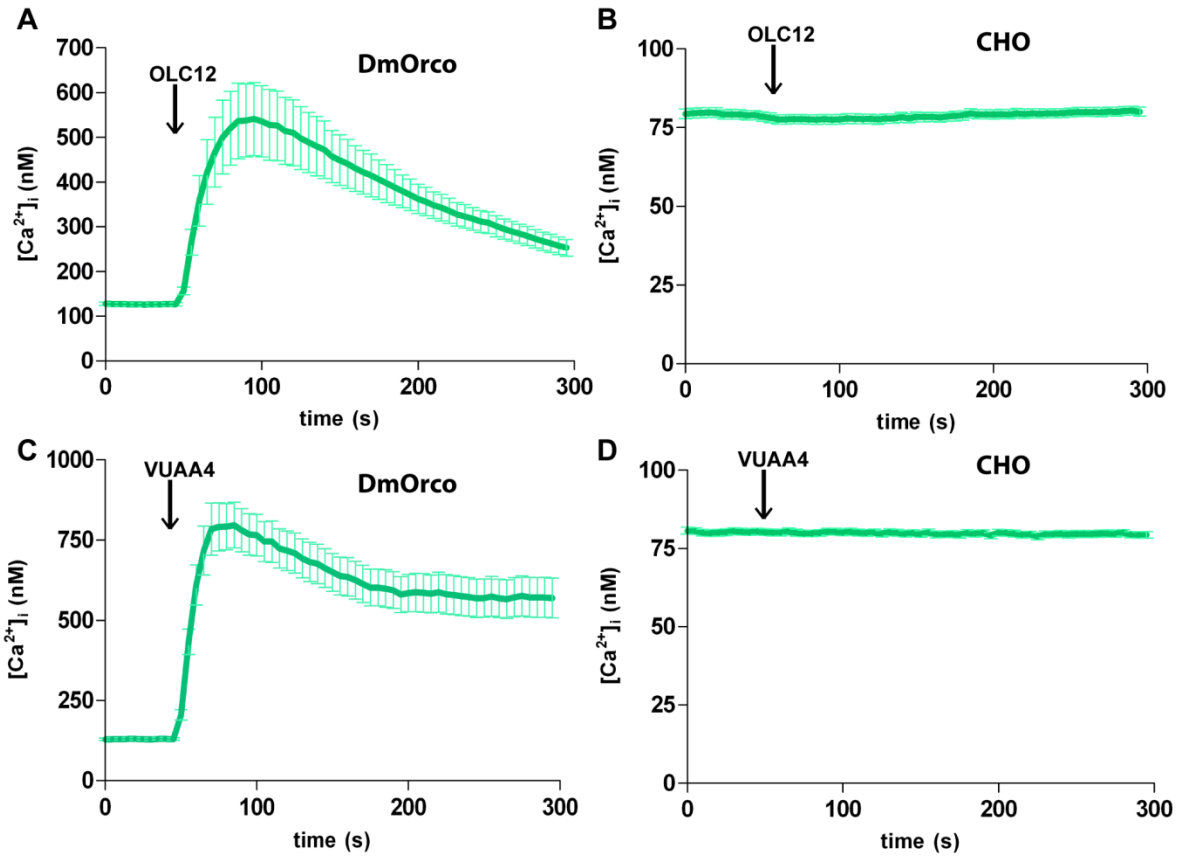

Fig. 11 | Kinetics as well as magnitude of DmelOrco regulated Ca^{2+}-responses monitored in CHO cells exposed to OLC12 or VUAA4 varied from characteristics of Ca^{2+}-signals controlled by MsexOrco observed in HEK293 cells. Effects of 100 µM OLC12 (A, B) or 10 µM VUAA4 (C, D) on CHO cells expressing DmelOrco (A,C) or on non-transfected CHO cells (B,D). Each graph represents the mean values for the different recordings gained by averaging the Ca^{2+}-concentrations of all signals at each time point. Compounds were applied after 50 s of recording. Analyzed cells (A) n=49, (B) n=52, (C) n=46 and (D) n=52.

3.3 Effects of OLC12 and VUAA4 on DmelOrco transfected CHO cells

To determine whether kinetics and size of the observed changes in intracellular Ca^{2+} levels are unique for MsexOrco, the same studies were performed on CHO cells stably transfected with DmelOrco (Fig. 11 A, C). The majority of CHO cells responded to applications of OLC12 or VUAA4 with a mean increase in $[Ca^{2+}]_i$ of 380 nM or 500 nM, respectively (Fig. 13 A1, B1). Presented with the stimuli cells directly responded with asymmetric Ca^{2+}-signals: Rising phases induced by OLC12 or VUAA4 lasted ~ 43 s and ~ 34 s on average, whereas falling

phases had a mean duration of ~ 202 s or 211 s. Ca^{2+}-levels of monitored, DmelOrco expressing CHO cells did not reach baselines after application of the agonists (Fig. 11 A, C). Considering the concentrations of OLC12 and VUAA4 these Ca^{2+}-profiles indicated a higher potency of VUAA4. In controls the compounds specificity was ensured by applying them to empty CHO cultures (Fig. 11 B, D). No changes in internal Ca^{2+}-levels were observed.

3.4 Characteristics of MsexOrco and DmelOrco controlled Ca^{2+}-responses to OLC12 or VUAA4

Direct comparison of Ca^{2+}-signals mediated by MsexOrco or DmelOrco and induced by the respective agonists indicate significant differences in duration and magnitude. DmelOrco transfected CHO cells displayed overall significantly higher mean increases in $[Ca^{2+}]_i$ than HEK293 cells expressing MsexOrco (Fig. 13 A1, B1). For a deeper insight into the kinetics of all monitored reactions induced by OLC12 or VUAA4, the measured decay phases were analyzed and their τ values calculated (Eq. 1.2, Eq. 1.3 Fig. 12). Thus, reaction rate of the falling phase depends only on the concentration of Ca^{2+} which in turn is regulated via various processes such as inactivation of cation channels, sequestration into internal stores or cellular removal via plasma membrane Ca^{2+}-ATPases (PMCAs). T increased with peak values in Ca^{2+}-concentration, mirroring prolonged falling phases. HEK293 cells stably transfected with MsexOrco exhibited relatively weak changes in intracellular Ca^{2+}-levels (Fig. 13) and τ values differed significantly from values in DmelOrco transfected CHO cells (Fig. 12). Hence responding HEK293 cell returned more rapidly to a pre stimuli status.

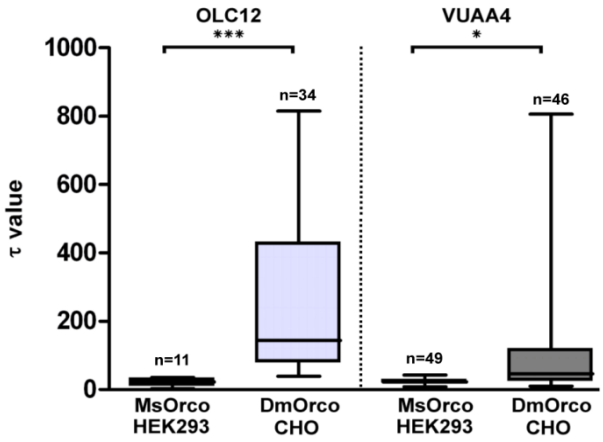

Fig. 12 | Decay phases of MsexOrco or DmelOrco mediated Ca^{2+}-responses varied significantly from each other. CHO cells stably transfected with DmelOrco needed more time to restore pre stimulus Ca^{2+}-concentrations than HEK293 cells expressing MsexOrco. Box plots illustrating calculated τ values of calcium-signal kinetics. Significant differences are indicated by asterisks (***P< 0.001, *P< 0.05; Student t-test, Mann-Whitney test).

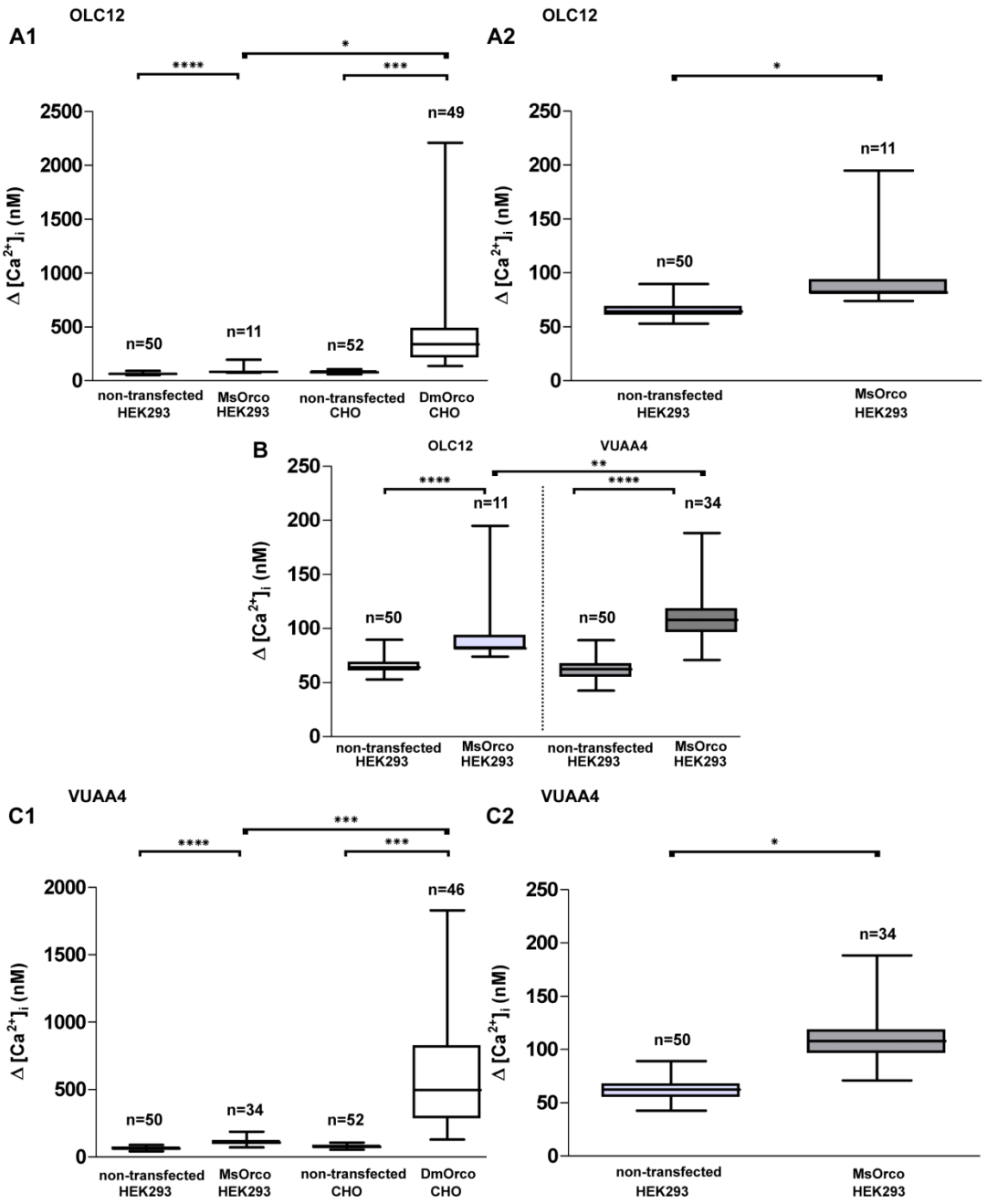

Fig. 13 | Cells stably transfected with Orco responded to applications of both Orco agonists OLC12 and VUAA4 with an increase in free intracellular Ca^{2+}-levels ($[Ca^{2+}]_i$). The rise in $[Ca^{2+}]_i$ under influence of the compounds varied significantly from responses of non-transfected cells. (A-C) Box plots depict the mean increase in free $[Ca^{2+}]_i$ after stimulation with 100 µM OLC12 or 10 µM VUAA4. (A1-A2) Mean increase in free $[Ca^{2+}]_i$ in the presence of OLC12. (A2) Magnification of the MsexOrco/HEK293 dataset from A1. (B) Comparison of $\Delta[Ca^{2+}]_i$ values mediated by MsexOrco and triggered by OLC12 respectively VUAA4. (C1-C2) Mean increase in free $[Ca^{2+}]_i$ in the presence of VUAA4. (C2) Magnification of the MsOrco/HEK293 dataset from C1. Significant differences are indicated by asterisks (A1-2, C1-2: ****P < 0.0001, ***P< 0.001, *P< 0.05, Kruskal-Wallis test; **P< 0.01, Mann-Whitney test).

3.5 *In vivo* patterns of agonist induced Ca^{2+}-signaling in HEK293 cells

We next focused on the patterns of OLC12 or VUAA4 triggered and MsexOrco controlled changes in intracellular Ca^{2+}-distribution. Fig. 14 illustrates calcium imaging recordings of representative, Fura-2 AM loaded HEK293 cells before as well as after control applications and responding to the tested compounds. Somata and cell extensions were fully stained. Depending on the utilized Orco agonist, cells exhibited different dynamics of induced Ca^{2+}-signals. In cells exposed to OLC12 increased Ca^{2+}-concentrations were first observed at cellular protrusions. Starting there, rises in Ca^{2+}-levels spread through the whole cell body in a few seconds (~ 5 s). Peaks in $[Ca^{2+}]_i$ (Fig. 14, upper panel) were found opposite to the signal's origin. In contrast to these results, VUAA4 directly elicited a substantial, global change in $[Ca^{2+}]_i$ (Fig. 14, lower panel). The origin of $[Ca^{2+}]_i$ rises resides thereby in the somata's center.

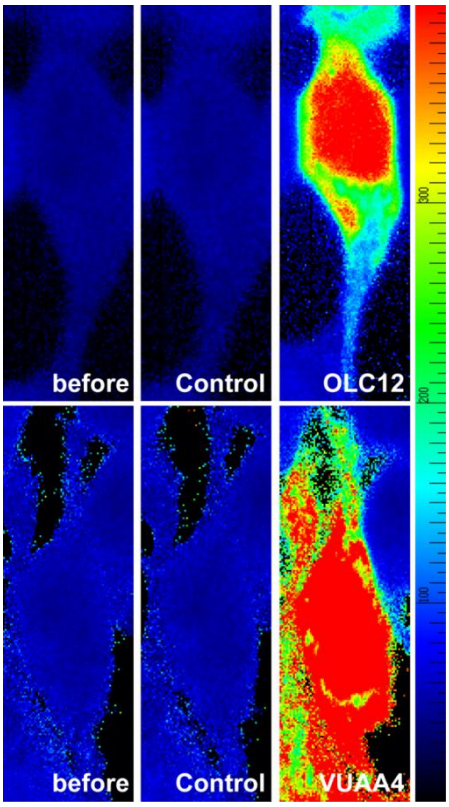

Fig. 14 | MsexOrco mediated and OLC12 or VUAA4 induced Ca^{2+}-changes differ not only in kinetics and magnitude, but also in their cellular distribution. Images from calcium imaging recordings of HEK293 cells stably transfected with MsexOrco before and after application (50 s) of either buffer, OLC12 or VUAA4. Pictures were taken when the cell's response reached peak levels (50 s control, VUAA4; 60 s OLC12). Scale bar 0-400 nM $[Ca^{2+}]_i$.

3.6 Composition of OLC12 induced Ca^{2+}-responses in DmelOrco transfected CHO cells

After we had gained insight into the Ca^{2+}-signal's distribution *in vivo*, we wanted to know whether or not internal Ca^{2+}-pools are involved in the generation of Orco's responses to stimuli. As expression levels of MsexOrco in our HEK293 cells were quite low, DmelOrco transfected CHO cells were used to have

a higher output in the following study. Cells were pretreated with buffer solutions containing 100 µM ryanodine or 10 µM dantrolene, prior to application of 100 µM OLC12 (Fig. 15 A, B). Both agents prevent intracellular Ca^{2+}-release by inhibition of ryanodine-receptors (RyRs) (Fig. 15 A, B). In controls monitored cells did not show any reaction to the used drugs alone. However, once preincubated cells were exposed to the agonist, they responded in a distinct lesser manner than without ryanodine or dantrolene treatment (Fig. 15 A, B). While both substances had comparable inhibiting effects on OLC12 triggered shifts in $[Ca^{2+}]_i$ (Fig. 16 C, D), they displayed noteable differences in their falling phase kinetics (Fig. 16 A, B). These findings depict that dantrolene and ryanodine might have blocked RyRs to a varying extent. Alternatively, dantrolene could have inhibited different, unidentified intracellular elements than ryanodine as mechanisms underlying dantrolene's action are not completely understood yet (Krause et al., 2004). However, obtained data revealed Orco mediated Ca^{2+}-signaling can be modulated by RyR antagonists. This modulating effect might have been caused by the lack of involvement of inner Ca^{2+}-stores or by an actual inhibition of DmelOrco itself. In order to further clarify whether intracellular Ca^{2+}-pools contribute to the generation of DmelOrco mediated Ca^{2+}-signals, cells were preincubated 40 min in 10 µM thapsigargin before applying OLC12. Thapsigargin blocks the sarco-endoplasmic reticulum Ca^{2+}-ATPase (SERCA) and causes thereby a depletion of intracellular Ca^{2+}-stores. If internal Ca^{2+}-pools

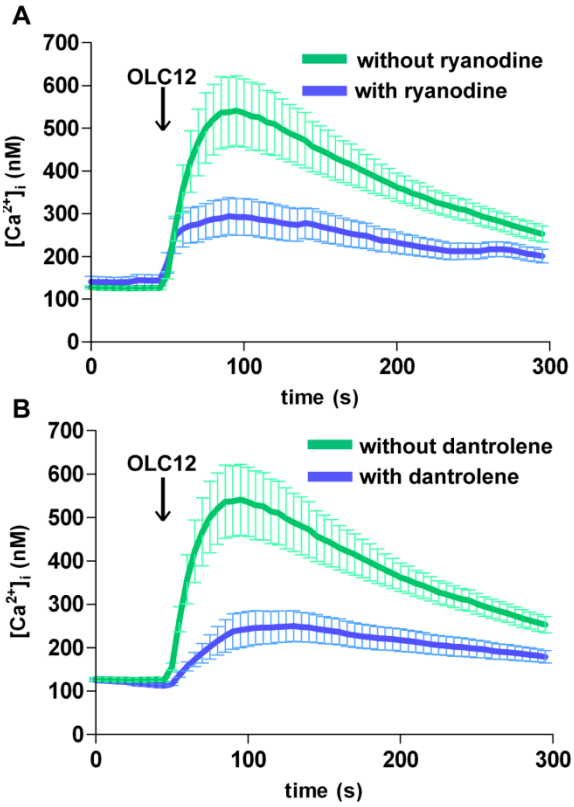

Fig. 15 | The presence of either ryanodine or dantrolene alters amplitude and kinetics of OLC12 triggered and DmelOrco mediated Ca^{2+}-responses. Effects of 100 µM ryanodine (A) or 10 µM dantrolene (B) on CHO cells stably transfected with DmelOrco. Each graph represents the mean values for the different recordings gained by averaging the Ca^{2+}-concentrations of all signals at each time point. Application of ryanodine or dantrolene after 25 s and addition of OLC12 after 50 s of recording. Analyzed cells (A) n=21 and (B) n=75.

are depleted and OLC12 elicits an increase in $[Ca^{2+}]_i$ comparable to Ca^{2+}-responses of untreated CHO cells, it is most likely that ryanodine and dantrolene serve as inhibitors of DmelOrco. Unexpectedly OLC12 failed to trigger any changes in $[Ca^{2+}]_i$-levels in thapsigargin treated cells (Fig. 17 A).

Due to the blocking of SERCAs, Ca^{2+} accumulated in the cell cytoplasm. Under these circumstances an involvement of intracellular Ca^{2+}-stores was foreclosed and DmelOrco

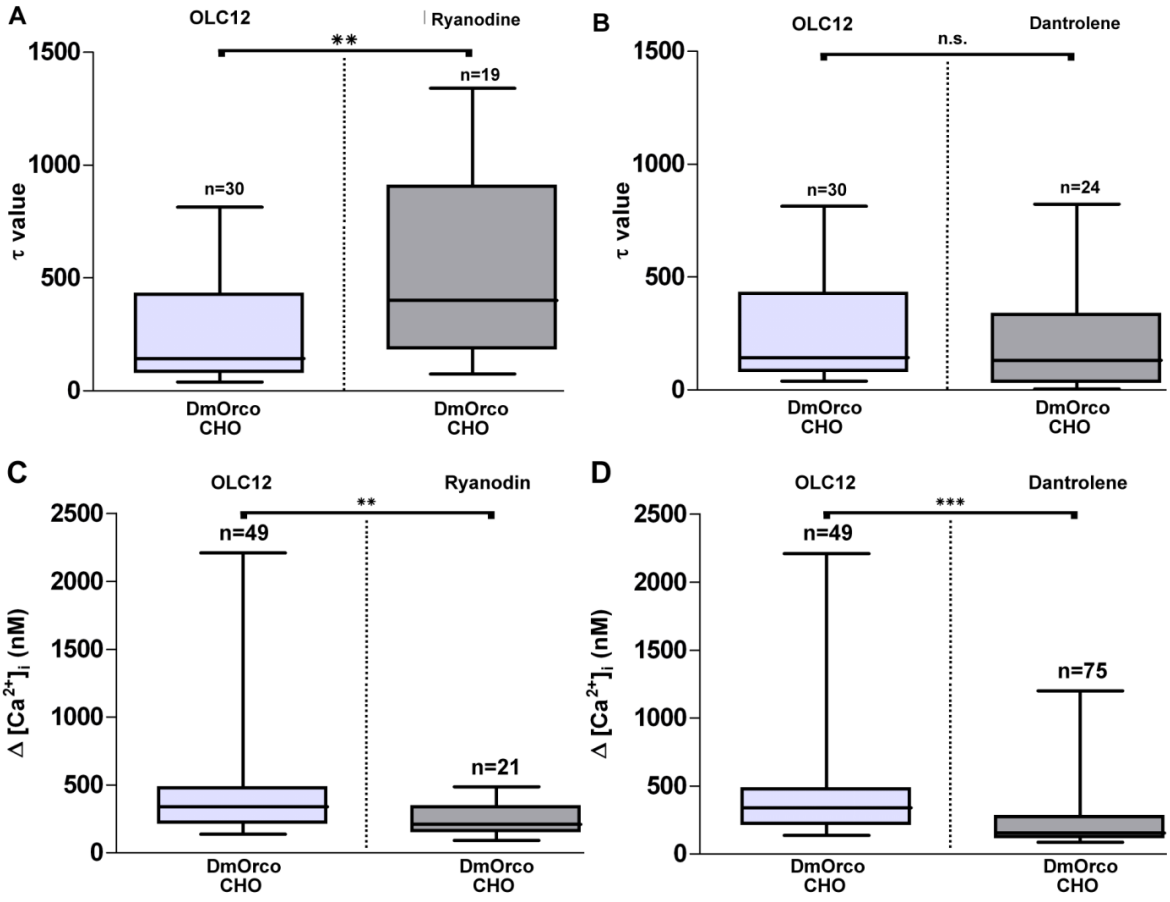

Fig. 16 | Ryanodine and dantrolene modify the falling phase kinetics of OLC12 induced and DmelOrco controlled Ca^{2+}-signals. Moreover, the ryanodine receptor antagonists have distinct depressing effects on the amplitude of triggered Ca^{2+}-responses. (A-B) Box plots representing calculated τ values of calcium imaging recordings. (C-D) Box plots show the mean increase in free intracellular Ca^{2+}-concentration $[Ca^{2+}]_i$ after stimulation with 100 µM OLC12 following prior applications of 100 µM ryanodine or 10 µM dantrolene. (A-D) Significant differences are indicated by asterisks (A-B: **P< 0.01, n.s. = not significant, Student t-test; C-D: ***P< 0.001, **P< 0.01, Mann-Whitney test).

might have been inactivated. To address this problem high Ca^{2+}-concentrations close to the plasma membrane were mimicked by exposing cells to 1 µM ionomycin prior to applications of OLC12 (Fig. 17 C). Application of ionomycin directly led to a severe increase in $[Ca^{2+}]_i$-levels. Peak values in Ca^{2+}-concentrations were first followed by a rapid decay which then gave way to a more steady falling phase after reaching $[Ca^{2+}]_i$ of 350-300 nM.

Before Ca^{2+}-concentrations reached pre stimulus levels, addition of OLC12 triggered a transient and very small increase in $[Ca^{2+}]_i$. This second rising phase led to a final falling

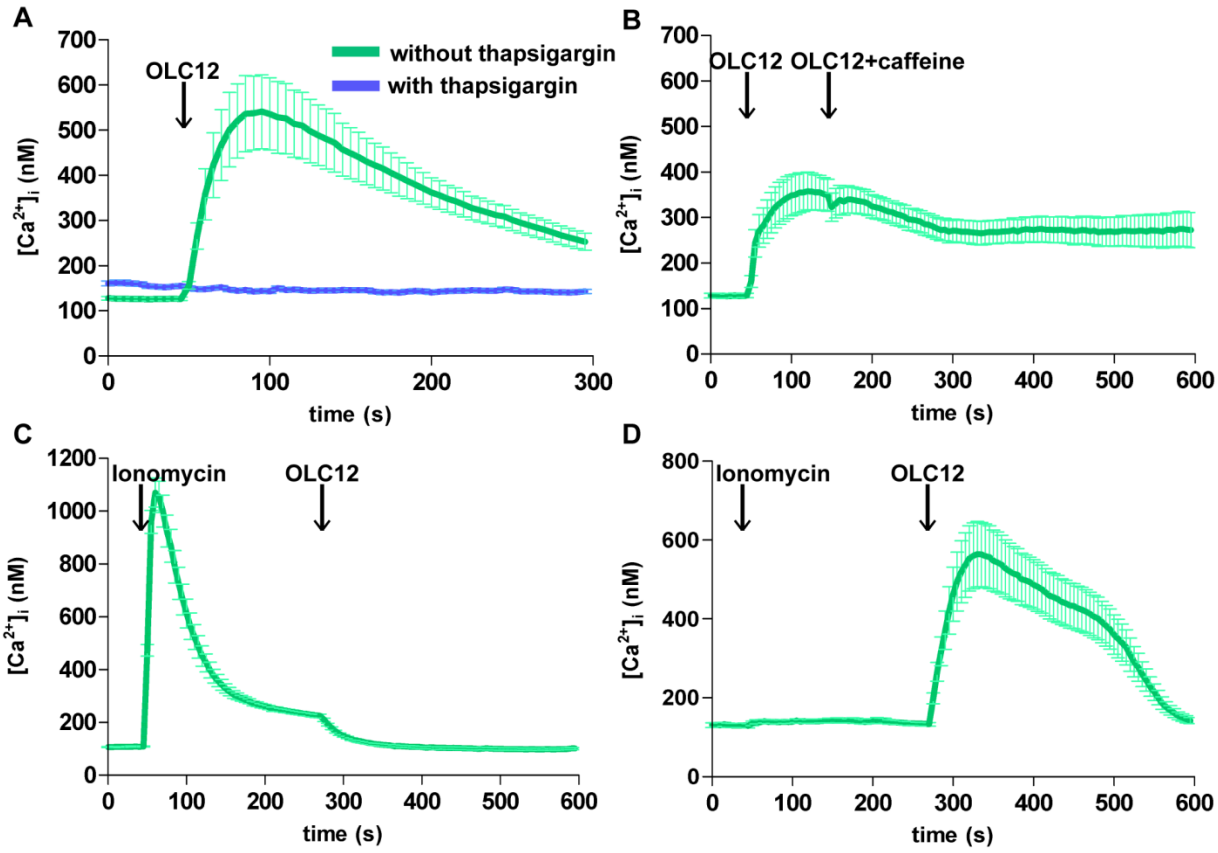

Fig. 17 | The Orco agonist OLC12 fails to elicit Ca^{2+}-responses in the presence of high intracellular Ca^{2+}-concentration ($[Ca^{2+}]_i \geq 190$ nM). Forced activation of ryanodine receptors via caffeine, i.e. Ca^{2+}-release from internal stores, did not increase the magnitude of OLC12 initiated and Orco mediated Ca^{2+}-signals. (A) Application of 100 µM OLC12 did not trigger changes in $[Ca^{2+}]_i$ after 40 min of incubation in 100 µM thapsigargin. (B) Effects of 20 mM caffeine on CHO cells stably transfected with DmelOrco. Application of OLC12 after 50 s and addition of caffeine plus OLC12 after 125 s of recording. (C-D) Effects of 1 µM (C) or 100 nM (D) ionomycin on CHO cells stably transfected with DmelOrco. Application of ionomycin after 50 s and addition of OLC12 after 275 s of recording. Analyzed cells (A) n=52, (B) n=17, (C) n=19 and (D) n=11. (A-D) The graphs represent the mean values for the different calcium imaging recordings gained by averaging the Ca^{2+}-concentrations of all signals at each time point.

phase, in which $[Ca^{2+}]_i$-base levels were restored. Ionomycin concentrations of 100 nM elicited only small changes in $[Ca^{2+}]_i$ and subsequent applications of OLC12 once again induced characteristic Ca^{2+}-signals comparable to response profiles of untreated CHO cells (Fig. 17 D). We now had evidence that DmelOrco is inactivated in the presence of high intracellular Ca^{2+}-levels. To further clarify whether ryanodine and dantrolene are yet unknown antagonists of Orco, we addressed again elements of intracellular Ca^{2+}-induced Ca^{2+}-release (CICR) by using 20 mM caffeine (Fig. 17 B).

Caffeine is a RyR agonist and mimicks CICR in various cell types. If internal Ca^{2+}-stores are involved in Orco initiated Ca^{2+}-responses, simultaneous applications of caffeine and OLC12 should induce evidently higher Ca^{2+}-signals than OLC12 addition alone. Monitored cells did not show an increase in $[Ca^{2+}]_i$-peak values in the presence of both drugs (Fig. 17 B). Kinetics were comparable to recordings with OLC12 application alone (Fig. 10, Fig. 17 B).

Taken together, the key question of a possible involvement of internal Ca^{2+}-stores in generation of DmelOrco regulated Ca^{2+}-signals or of a putative DmelOrco inhibiting effect of ryanodine and dantrolene requires further investigation to verify either one of the hypotheses. Furthermore DmelOrco's function and activation level seem to depend on intracellular Ca^{2+}-concentration.

3.7 *In vivo* permeability for Orco agonists in *Manduca sexta*

Since we had confirmed earlier that OLC12 and VUAA4 are valuable agonists of MsexOrco, we now had a starting point to modulate Orco's level of activation in *Manduca sexta in vivo*. We planned to perform wind tunnel behavioral studies in order to track and record Orco mediated changes in characteristics of the insect's olfactory system. In advance we had to find a way for a noninvasive method of presenting the ORNs with OLC12 or VUAA4 over a longer period of time without additionally affecting the animal. One approach was to incubate the antennae of adult *M. sexta* individuals in sensillum lymph Ringer with the agonist prior to the wind tunnel experiments. The other approach was to inject the biological agents directly into the hemolymph system of the hawk moth's antennae. To evaluate whether substances with structures like OLC12 or VUAA4 applied in these two manners can elicit changes in the olfactory system, tip recordings were performed. As OLC12 and VUAA4 resulted from minor alterations to the structure of the Orco activator VUAA1, they share highly similar structures

with this compound. Due to this fact and the reason that we knew from earlier studies how VUAA1 affects the spontaneous AP-generation of ORNs *in vivo*, we ran our experiments with VUAA1 instead of OLC12 or VUAA4. When 100 µM or 1 mM VUAA1were added to the hemolymph Ringer of the recording electrode slipped over the truncated antenna's tip, there was no significant increase in the spontaneous activity level of monitored ORNs (Fig. 18). These results indicate that antennal tissue is impermeable to VUAA1 and most likely to VUAA1 related drugs.

One-hour incubation of intact moth antennae in sensillum lymph Ringer containing 100 µM VUAA1 did also not affect the spontaneous activity patterns of recorded ORNs (Fig. 18). Thus VUAA1 either could not pass through the sensilla's pores or the incubation time was too short for VUAA1 to diffuse into the sensilla's cavity and activate Orco. Only when the sensilla's tip was truncated and the recording electrode backfilled with sensillum lymph Ringer containing 100 µM VUAA1 was slipped over the open end, the recordings displayed a significant rise in spontaneous activity levels (Fig. 18).

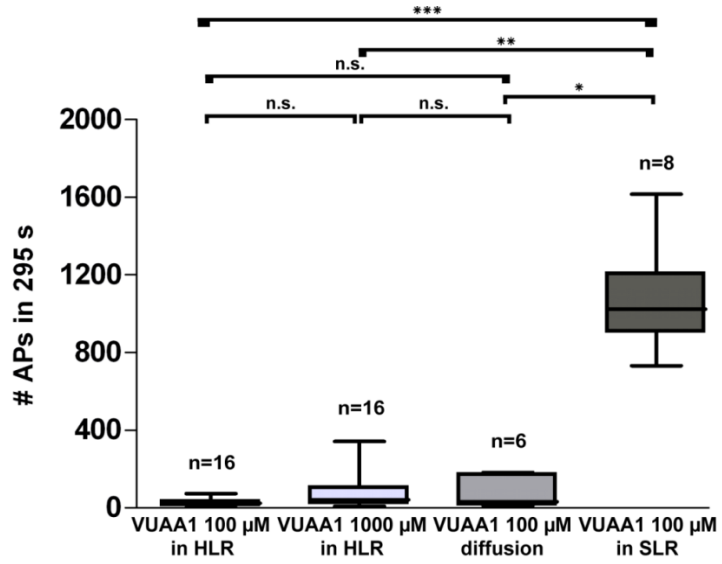

Fig. 18 | Neither incubation of *M. sexta*-antennae in sensillum lymph Ringer (SLR) containing VUAA1 nor addition of this compound to the hemolymph Ringer (HLR) modulates the spontaneous activity of olfactory receptor neurons in tip recordings. Box plots depict spontaneous activity levels of olfactory receptor neurons during tip recordings of 300 s. Only addition of VUAA1 directly to the SLR changed the spontaneous activity of recorded ORNs. Significant differences are indicated by asterisks (***P < 0.001, **P < 0.01, *P < 0.05, n.s. = not significant; One-Way-Anova).

4 Discussion

Decades of research on insect odor transduction have revealed various elements involved in events occurring before, while and upon ligand-binding to olfactory chemosensory receptor complexes. However, there are still a lot of unresolved issues regarding mechanism underlying olfactory signal transduction. Although there is plenty of evidence that the highly conserved Orco has a key role in insect olfaction besides membrane trafficking and membrane maintenance of ORs, little is known about the co-receptor's characteristics and the mechanisms by which it takes part in olfactory signal transduction.

In this thesis, calcium imaging measurements and tip recordings were used to evaluate the range of application for the recently identified Orco agonists OLC12 and VUAA4 (Jones et al., 2011; Chen & Luetje, 2012; Taylor et al., 2012) in the characterization process of *M. sexta*'s Orco ortholog, MsexOrco. We not only established OLC12 and VUAA4 as agonists of heterologously expressed MsexOrco, but also confirmed that VUAA4 is the more potent agonistic drug of both tested substances (Taylor et al., 2012). In *in situ* tip recordings, we analyzed the permeability of antennal tissue for the first of its class identified, specific Orco agonist VUAA1, which is a structural analogue of OLC12 and VUAA4 (Jones et al., 2011). Data from different experiments indicate that VUAA1 cannot unhindered cross the assembly of cells and extracellular matrix in antenna from *M.* sexta (Fig. 18). Furthermore, OLC12 and VUAA4 were used to learn more about key features of Orco regulated rises in intracellular Ca^{2+}-concentration. In the heterologous expression system of CHO cells, we investigated a putative contribution of internal Ca^{2+}-stores to DmelOrco mediated Ca^{2+}-signals and determined whether or not ryanodine as well as dantrolene are qualified for an inhibition of Orco activity. Although these hypotheses were not finally verified, valuable evidence for a correlation of Orco activity and intracellular, free Ca^{2+}-concentration was obtained. According to our findings DmelOrco is inactivated in the presence of highly elevated Ca^{2+}-levels.

4.1 Expression and plasma membrane incorporation of MsexOrco is impaired in HEK293 cells

MsexOrco was stably expressed in HEK293 cells and the co-receptors heterologous expression levels as well as its membrane association were examined via immunohistochemistry preliminary to further experiments. The low quantity of Orco-like

immunoreactivity in cell culture, indicated faint heterologous expression of the co-receptor. An explanation for this finding might be the previously reported ability of (heterologously) expressed Orco to form oligomeric membrane pores of unknown stoichiometry which are leaky cation channels (Wicher et al., 2008; Jones et al., 2011, 2012; Nolte et al., 2013). A non-regulated, constitutive cation-influx via moderate or high levels of leaky ion channel-forming Orco-subunits could lead to a cell's death by changing the inhomogeneous distribution of Na^+, K^+ and particular Ca^{2+} between cytosol and extracellular fluid. Alterations in the strictly defined extra- and intracellular ion composition maintained by the plasma membrane and its incorporated transport systems, impair the continuity of physiological processes and have a tremendous impact on a cell's life span. Thus, only HEK293 cells exhibiting low expression levels of Orco or no expression at all would survive and the cell culture's majority would show no Orco-like immunoreactivity.

Besides the faint expression of MsexOrco in the heterologous HEK293 cell culture, comparison of Orco and WGA immunostaining intensity profiles provided evidence that the co-receptor is predominately present in the HEK293 cells' cytosol and only rarely incorporated into the plasma membrane. *In vivo* Orco passes the endomembrane system (Benton et al., 2006) of odorant receptor neurons in anterograde direction and eventually reaches its final destination in the plasma membrane. According to a recent study (Nolte et al., 2013) and based on MsexOrco's observed sparse membrane association, we assume a lack of essential elements for proper membrane trafficking of the co-receptor in the vertebrate HEK293 cell system. These crucial elements might be chaperones for correct protein folding or proteins involved in the secretory pathway of Orco.

Due to Orco's impaired membrane incorporation in HEK293 cell culture and the putative lethality of its overexpression, use of an inducible expression system as well as fluorescence activated cell sorting (FACS) would be of great benefit for future investigations on MsexOrco's characteristics. While the transcription of the *orco* gene is repressed in the absence of an inducer, survival of cells stably transfected with MsexOrco is insured (Personal communication with J. A. Corcoran, The New Zealand Institute for Plant & Food Research Limited, Auckland, New Zealand). Subsequent sorting of successfully transfected cells via fluorescent protein tags would then allow maintenance of cell cultures with high expression levels of the gene of interest. Anyhow, the use of a heterologous expression system goes along with the risk of a missing molecular translational machinery and an absence of cellular elements necessary for correct protein folding and translocalization.

4.2 OLC12 and VUAA4 are agonists of MsexOrco

Despite MsexOrco's faint heterologous expression and its rare membrane association, we were able to trigger significant rises in intracellular Ca^{2+}-concentration via applications of the recently synthesized and identified agents OLC12 or VUAA4 (Chen & Luetje, 2012; Taylor et al., 2012), respectively. Using different concentrations of working solution, we compared the activity of OLC12 and VUAA4 by AUC-analyses of the monitored Ca^{2+}-responses. VUAA4 was considerably more potent than OLC12. Both compounds are capable of gating MsexOrco and thus valuable tools for its characterization, as described for other members of the Orco family (Jones et al., 2011, 2012; Chen & Luetje, 2012; Taylor et al., 2012). Nevertheless, VUAA4's higher potency of activation makes this drug the more efficient agonist.

4.3 Cellular distribution of MsexOrco mediated rises in $[Ca^{2+}]_i$

Examination of *in vivo* patterns of OLC12 or VUAA4 induced and MsexOrco regulated changes in intracellular Ca^{2+}-distribution indicated different temporal dynamics as well as spatial non-uniformities of triggered $[Ca^{2+}]_i$-rises. One explanation for disparities in temporal dynamics of MsexOrco-controlled Ca^{2+}-signals could be the above described difference in potency of OLC12 and VUAA4. Hence, both agonists had the same amount of time to spread through the bath and reach the HEK293 cells, but due to VUAA4's higher potency it required less VUAA4-molecules to elicit a global Ca^{2+}-response in encountered cells (Taylor et al., 2012). Furthermore, MsexOrco's expression levels and amount of membrane incorporation could have differed between analyzed cells, mediating a different Ca^{2+}-influx, independent of the applied agonist. Additional to the unpredictable aspects of MsexOrco's expression level and membrane incorporation, calcium-ions entering the cell accumulate transiently near the plasma membrane, diffuse through the cytosol and eventually might have initiated CICR to a magnitude that naturally differs from cell to cell (Brady et al., 1994)

Calcium imaging measurements illustrating the cellular distribution of MsexOrco mediated $[Ca^{2+}]_i$-rises convey the impression of peak values in intracellular Ca^{2+}-concentration proximal to the cell's nucleus (Fig. 14). This observation might be due to Ca^{2+}-release from the ER's vast system of membrane tubules and sacs surrounding the nucleus, regulated via MsexOrco ion channels incorporated into the ER's membrane (German et al., 2013) or via CICR.

Alternatively, this finding could be an artifact caused by the experimental setup. HEK293 cells are complex, three-dimensional structures and during our calcium imaging recordings fluorescence signals from planes other than the actual focal plane were likewise detected. Spatial summation of these fluorescence ratios at protruding cell regions might have created a heat map which depicts a false, striking non-uniformity in dispersion of internal Ca^{2+}-levels. Moreover, besides variations in expression level and quantity of membrane association, distribution of Orco ion channels in the plasma membrane could have differed. According to the fluid mosaic model (1976) by S. J. Singer and G. Nicolson, membrane proteins can float two-dimensionally in the lipid layer of biological membranes. Thus, if not restricted to a certain area, Orco oligomers could move freely in the plasma membrane and would be distributed randomly over the whole cell body. Since, our recordings are only snap shots in time, non-uniformities in cellular patterns of $[Ca^{2+}]_i$-rises between stimulation with OLC12 or VUAA4 might be partially caused by fortuitous dispersion of Orco channels in the monitored cells' plasma membrane.

4.4 Differences in magnitude and kinetics of MsexOrco or DmelOrco mediated Ca^{2+}-signals

In order to evaluate whether kinetics and amplitude of OLC12 or VUAA4 induced Ca^{2+}-signals are mediated by the substances themselves or by MsexOrco, we compared agonist triggered Ca^{2+}-responses of HEK293 cells expressing MsexOrco with responses of CHO cells stably transfected with DmelOrco. Analysis of the mean increase in $[Ca^{2+}]_i$ upon exposure to either one of the compounds and falling phase kinetics of the recorded Ca^{2+}-profiles revealed significant differences between magnitude and duration of MsexOrco or DmelOrco initiated Ca^{2+}-signals. Disregarding the fact that the two members of the Orco family were expressed in different expression systems, with varying quantity, but considering that all other experimental parameters were the same, our findings point to a variation in the cation conductivity of MsexOrco and DmelOrco. However, each heterologous expression system together with the putative different expression levels of the Orco orthologs affected most likely the Ca^{2+}-responses kinetics in a non-negligible manner. Since the majority of CHO cells stably transfected with DmelOrco reacted to the presence of OLC12 or VUAA4 with the generation of Ca^{2+}-responses, it is relatively safe to assume a high expression level of DmelOrco in our CHO cell culture. Recent unpublished data from patch clamp experiments

on cells expressing MsexOrco or DmelOrco provides evidence that Orco membrane pore units are capable of linking their activity for a synchronized response and that Orco ion channels are oligomers formed by several Orco units. Thus, availability of Orco monomers would have greatly affected these processes and most probably alter a cell's Ca^{2+}-signal upon exposure to OLC12 or VUAA4, respectively. Furthermore, CHO and HEK293 cells not only possess a different set of ion channels incorporated in their plasma membrane but also express an alternative variety of subcellular compartment ion pores (Suda et al., 1997; Tong et al., 1999; Yu & Kerchner, 1998). To a lesser extent than variations in Orco's expression level, these different initial conditions could have affected kinetics and amplitude of triggered Ca^{2+}-signals by additional Orco activation-dependent Ca^{2+}-fluxes through the plasma membrane. Depending on the used cell system, a release of calcium-ions from internal pools as a result of Orco mediated rises in $[Ca^{2+}]_i$ might have contributed to the eventually recorded Ca^{2+}-response in a varying ratio. Therefore, non-uniformities in kinetics and magnitude of MsexOrco or DmelOrco mediated intracellular Ca^{2+}-increase might not be caused by the orthologs' characteristics but rather be due to the different expression level of the relative Orco protein and conceivably due to variations in the expression systems characteristics. Future studies performed on the same heterologous cell system, should be able to determine whether OLC12 and VUAA4 induce comparable, Orco mediated responses.

4.5 Do ryanodine and dantrolene have inhibiting effects on DmelOrco formed ion channels?

In line with recently published findings and results (Stengl, 2010; Jones et al., 2011; Chen & Luetje, 2012; Nolte et al., 2013), our data indicate that Orco subunits form homomeric membrane ion channels which possess ligand-binding sites and operate as cation channels. The Orco specific agonists were used to investigate a putative involvement of internal Ca^{2+}-pools in the generation of Orco mediated Ca^{2+}-responses. Ryanodine and dantrolene had inhibiting effects on kinetic and amplitude of OLC12 triggered Ca^{2+}-signals. These findings promoted the assumption of an Orco-activation dependent internal Ca^{2+}-release initiated by Orco regulated rises in $[Ca^{2+}]_i$ or Orco induced production of second messenger such as IP_3. Furthermore, Orco ion channels might reside in the ER membrane, regulating Ca^{2+}-release from this cellular compartment themselves (German et al., 2013). Simultaneous

application of the RyR agonist caffeine together with OLC12 did not induce more prominent Ca^{2+}-responses than OLC12 stimulation alone. Although this observation might argue against an involvement of internal Ca^{2+}-pools at first, it is more likely that the present Orco ion channels might have been inactivated due to elevated $[Ca^{2+}]_i$-level mediated by prior OLC12 application. Since one our data hinted to an inhibiting effect of ryanodine and dantrolene on Orco's activity, this key question was further investigated. We predicted, in the absence of the putative inhibiting acting ryanodine and dantrolene, OLC12 should have been able to induce Orco-controlled Ca^{2+}-influx while intracellular Ca^{2+}-pools were depleted via thapsigargin treatment. But in fact, we did not observe any shifts in $[Ca^{2+}]_i$ after application of the Orco agonist. These findings did not help to conclusively clarify whether the RyR antagonists ryanodine and dantrolene are yet unknown blocker of Orco orthologs. The data rather indicated that intracellular Ca^{2+}-stores contribute to the generation of Orco regulated Ca^{2+}-responses, as depletion of these pools apparently prevented Ca^{2+}-rises upon Orco stimulation. Future experiments with calcium free extracellular media during recordings should finally elucidate whether internal Ca^{2+}-stores are essential for Orco mediated Ca^{2+}-signaling. If this is the case, we should be able to record Ca^{2+}-responses upon Orco activation even though the extracellular solution is Ca^{2+}-free.

4.6 Function and activation level of DmelOrco formed ion channels depend on intracellular Ca^{2+}-concentration

Data from earlier experiments provided evidence that Orco ion channels might be inactivated via highly elevated internal Ca^{2+}-levels. We mimicked accumulation of calcium-ions in close range to the plasma membrane, applying ionomycin to monitored cell cultures. While application of 1 µM ionomycin directly led to a substantial increase in intracellular Ca^{2+}-concentration, a following OLC12 stimulus failed to elicit a notable rise in internal Ca^{2+}-levels. On closer examination of the ionomycin initiated Ca^{2+}-profile, we spotted a small increase in $[Ca^{2+}]_i$ during the signal's falling phase, upon addition of OLC12. This finding is in line with the prior observation of an inactive Orco during high cytosolic concentration of Ca^{2+}, but also added a new level of complexity to our preliminary presumption. Therefore, activity of phospholipase C and rising Ca^{2+}-levels might have altered PKC's conformation to its active form (Sargsyan et al., 2011). Ca^{2+}-influx depending shifts in the transmembrane potential

together with phosphorylation events via PKC could have gated Orco channels, further elevating intracellular Ca^{2+}-concentration. Increased cytosolic Ca^{2+}-levels would have led to formation of active calmodulin-complexes which directly or indirectly via effectors arrested gated Orco ion channels in a negative feedback loop. Since the decrease in internal Ca^{2+}-concentrations slowed down after a rapid falling phase, some Orco ion channels might have remained open. Activation of these gated Orco oligomers by application of OLC12 might thereupon have triggered a new Ca^{2+}-increase. Transient accumulation of calcium-ions proximal to the plasma membrane and/or two stage activation of Orco then abruptly inactivated multiple ion channels, restoring $[Ca^{2+}]_i$-base levels. Taken together, DmelOrco's function as well as its conductive properties seem to depend on cytosolic Ca^{2+}-concentration and might be modulated by a double switch progress. This two step event could be implemented via voltage and phosphorylation depending changes in the channels' conformation together with binding of an allosteric effector. Certainly, future studies have to provide further proof for our double switch model.

4.7 VUAA1 cannot cross antennal tissue of *M. sexta* via diffusion

In a final series of experiments, we analyzed the *in vivo* cell permeability for VUAA1 and related compounds (OLC12, VUAA4) by performing tip recordings on antennae of male *M. sexta* adults. These trails were preliminary work for future planned, wind tunnel behavioral studies, in which we wanted to investigate whether or not interference of Orco's level of activity via its prior established agonists, modulates characteristics (e.g. frequency of odor sampling) of the insect's olfactory system (Stengl, 2010; Tripathy et al., 2010; Nolte et al., 2013). In two different approaches we either added varying concentration of VUAA1 to the HLR of the reference electrode, slipped over the antenna's truncated tip, or incubated the intact antenna in SLR containing VUAA1. Contrary to recordings in which VUAA1 was added directly to the SLR of the recording electrode (Nolte et al., 2013), neither approach triggered any significant rises in the spontaneous activity of monitored ORNs. Thus, VUAA1 was neither capable of passing through the trichoid sensilla's pores into its cavity and activate Orco, nor were the compound's molecules able to cross antennal tissue and its extracellular matrix such as the basal lamina which is secreted by epidermis as well as sheath cells isolating sensillum lymph and hemolymph from each other. One explanation might be, that the used incubation time was not long enough for VUAA1 to reach its final destination and

modulate Orco's activity level. Since odorants and pheromones bind to OBPs or PBPs in order to be translocated to their specific ORs and to cross the insect's aqueous body fluids (Kaissling, 2009), a lack of these, unique transporter proteins for VUAA1 might have drastically decreased its velocity of movement. Moreover, the compound's physiochemical properties probably prevented its passage through the extracellular matrix of encountered cells or perhaps the drugs translocalization across the lipid bilayer of the cell plasma membranes. Non-diffusible substances rely on the presence of membrane transport proteins in order to cross a plasma membrane. Some drugs are capable of using present transporters for their benefit by being recognized due to structural similarities with natural occurring compounds or nutrients (Bambeke et al., 2006). Our data not only indicates that VUAA1 and hence most likely also its related substances cannot diffuse across antennal tissue, but also that there is no alternative transport mechanism for its translocalization across plasma membranes.

5 Summary

Fourteen years ago Orco was discovered (Vosshall et al., 1999, 2000) as an ubiquitous factor in the olfactory system of insects. Since then the precise molecular mechanisms by which this co-receptor protein takes part in olfactory signal transduction are still unknown. At the moment there are three main conflicting hypotheses on Orco's role in affecting an insect's odor response. One assumption is that the olfactory co-receptor forms OR-Orco heteromers (Neuhaus et al., 2005; Benton et al., 2006), which are odor-gated ion channels and alter dose-dependent receptor potentials as well as AP-responses in behaving animals (Sato et al., 2008). Another hypothesis is that ORs are ionotropic, ligand-gated ion channels and that metabotropic activation of Orco leads to enhanced sensitivity of these channels (Olsson et al., 2011; Sargsyan et al., 2011; Wicher, 2008, 2013; Getahun et al., 2013). The third opinion suggests Orco is capable of constituting leaky ion channels of unknown stoichiometry on its own, thereby producing oscillations in the membrane potential (Stengl, 2010; Nolte et al., 2013). This renders ORNs sensitive to time frames of olfactory input and allows for temporal encoding (Stengl, 2010; Nolte et al., 2013).

To further enlighten Orco's part in the olfactory transduction cascade of insects it would be of great benefit to specifically activate or block its function. Recent studies (Jones et al., 2011, 2012; Chen & Luetje, 2012; Taylor et al., 2012) identified the substances OLC12 and VUAA4 as agonists of Orco in the insect species *Aedes aegypti*, *Anopheles gambiae*, *Culex quinquefaciatus*, *Drosophila melanogaster*, *Harpegnaths saltator*, *Heliothis virescens* and *Ostrinia nubilalis*.

In this study, via calcium imaging recordings, we were able to demonstrate that OLC12 and VUAA4 are feasible agonists of the ubiquitous olfactory co-receptor in *Manduca sexta* as well. Comparison of Ca^{2+}-signals triggered by these compounds and mediated by MsexOrco, indicated a considerable higher potency of VUAA4, making this substance the more efficient agonist. In tip recordings on trichoid sensilla of male *M. sexta* adults, the *in vivo* cell permeability for VUAA1 was analyzed. The results depict proof, that VUAA1 and therefore probably related compounds cannot cross antennal tissue via diffusion and that there is most likely no alternative transport system for its translocalization.

With the opportunity of altering Orco's activity level, we looked into a putative involvement of intracellular Ca^{2+}-stores in the generation of DmelOrco regulated Ca^{2+}-responses. Since our data was inconclusively, we could not finally elucidate whether there is an Orco-activation

dependent Ca^{2+}-release from internal stores. Also, it remains unresolved whether the RyR blocker ryanodine and dantrolene have inhibiting effects on the activity of Orco.

Our findings support the assumption that function and conductive properties of Orco depend on cytosolic levels of Ca^{2+}-ions and might be modulated by a two step event of changes in the transmembrane potential and phosphorylation processes together with binding of an allosteric ligand, eventually altering the membrane pore's conformation.

Taken together, this thesis supports the recent proposed model that Orco monomers form homomeric leaky ion channels which generate oscillations in a cell's spontaneous membrane potential (Stengl, 2010; Nolte et al., 2013). These ion channels are gated by activity of PLCs (Getahun et al., 2013; Sargsyan et al., 2011) together with rises in the intracellular Ca^{2+}-concentration and can be further activated upon ligand binding to an intrinsic allosteric pocket, while they are inactivated via a negative feedback loop during via elevated internal Ca^{2+}-levels.

6 Acknowledgments

I would like to thank Prof. Dr. Monika Stengl who initially introduced me to the field of Animal physiology and supervised me not only throughout my academic studies but also during the realization of this thesis. Also, I want to thank Prof. Dr. Bill S. Hansson and PD Dr. Dieter Wicher for giving me the opportunity to accomplish my thesis at the Max Planck Institute for Chemical Ecology. In particular, I appreciate the advice, support and encouragement PD Dr. Dieter Wicher granted me during my time in Jena and beyond. No matter which problems came up he was always open and helpful in his counsel.

Furthermore, I owe special thanks to Christopher König, Alexander Haverkamp, Oksana Tuchina, Latha Mukunda, Dr. Ewald Grosse-Wilde and my other co-workers at the MPI CE. The friendly and pleasant environment created by them, their encouraging words and their expert advice helped me realizing this work. I'm also very grateful to Sabine Kaltofen for taking care of cell culture and preparing the countless amount of cell covered cover slips.

Last but not least, special thanks go to Nico Funk, Achim Werckenthin, Andreas Nolte and Petra Gawalek who above all supported and encouraged me, accepting my insecurities.

7 References

Altner, H., & Prillinger, L. (1980). Ultrastructure of Invertebrate Chemo-, Thermo-, and Hygroreceptors and Its Functional Significance. *International Review of Cytology*, *67*, 69–139.

Benton, R., Sachse, S., & Vosshall, L. B. (2006). Atypical membrane topology and heteromeric function of *Drosophila* odorant receptors in vivo. *PLoS biology*, *4*(2), e20.

Benton, R., Vannice, K. S., & Vosshall, L. B. (2007). An essential role for a CD36-related receptor in pheromone detection in *Drosophila*. *Nature*, *450*(7167), 289–93.

Berridge, M. J. (1997). Elementary and global aspects of calcium signalling. *Journal of Physiology*, *499*(2), 291–306.

Boekhoff, I., Seifert, E., Goggerle, S., Lindemann, M., Kruger, B., & Breer, H. (1993). Pheromone-Induced Second-Messenger Signaling in Insect Antennae, *23*(7), 757–762.

Boekhoff, I., Strotmann J., Raming, K., & Tareilus et al. (1990). Odorant-sensitive phospholipase C in insect antennae, *2*(I), 49–56.

Bohbot, J. D., & Dickens, J. C. (2012). Odorant receptor modulation: ternary paradigm for mode of action of insect repellents. *Neuropharmacology*, *62*(5-6), 2086–95.

Brady, K. D., Wagner, K. a, Tashjian, a H., & Golan, D. E. (1994). Relationships between amplitudes and kinetics of rapid cytosolic free calcium fluctuations in GH4C1 rat pituitary cells: roles for diffusion and calcium-induced calcium release. *Biophysical journal*, *66*(5), 1697–705.

Breer et al. (1990). Rapid kinetics of second messenger formation in olfactory transduction. *Nature*, *345*, 65–68.

Chen, S., & Luetje, C. W. (2012). Identification of new agonists and antagonists of the insect odorant receptor co-receptor subunit. *PloS one*, *7*(5), e36784.

Clapham, D. E. (2007). Calcium signaling. *Cell*, *131*(6), 1047–58.

Clyne, P. J., Warr, C. G., Freeman, M. R., Lessing, D., Kim, J., & Carlson, J. R. (1999). A novel family of divergent seven-transmembrane proteins: candidate odorant receptors in Drosophila. *Neuron*, *22*(2), 327–38.

Couto, A., Alenius, M., & Dickson, B. J. (2005). Molecular, anatomical, and functional organization of the Drosophila olfactory system. *Current biology : CB*, *15*(17), 1535–47.

Deng, Y., Zhang, W., Farhat, K., Oberland, S., Gisselmann, G., & Neuhaus, E. M. (2011). The stimulatory Gα(s) protein is involved in olfactory signal transduction in *Drosophila*. *PloS one*, *6*(4), e18605.

Ditzen, M., Pellegrino, M., & Vosshall, L. (2008). Insect Odorant Receptors Are Molecular Targets of the Insect Repellent DEET. *Science*, *319*(5871), 1838–1842.

Dolzer, J. (2003). Adaptation in pheromone-sensitive trichoid sensilla of the hawkmoth *Manduca sexta*. *Journal of Experimental Biology*, *206*(9), 1575–1588.

Flecke, C., Dolzer, J., Krannich, S., & Stengl, M. (2006). Perfusion with cGMP analogue adapts the action potential response of pheromone-sensitive sensilla trichoidea of the hawkmoth *Manduca sexta* in a daytime-dependent manner. *The Journal of experimental biology*, *209*(Pt 19), 3898–912.

Forstner, M., Gohl, T., Gondesen, I., Raming, K., Breer, H., & Krieger, J. (2008). Differential expression of SNMP-1 and SNMP-2 proteins in pheromone-sensitive hairs of moths. *Chemical senses*, *33*(3), 291–9.

Gao, Q., & Chess, A. (1999). Identification of candidate *Drosophila* olfactory receptors from genomic DNA sequence. *Genomics*, *60*(1), 31–9.

German, P. F., Van der Poel, S., Carraher, C., Kralicek, A. V, & Newcomb, R. D. (2013). Insights into subunit interactions within the insect olfactory receptor complex using FRET. *Insect biochemistry and molecular biology*, *43*(2), 138–45.

Getahun, M. N., Olsson, S. B., Lavista-Llanos, S., Hansson, B. S., & Wicher, D. (2013). Insect Odorant Response Sensitivity Is Tuned by Metabotropically Autoregulated Olfactory Receptors. *PLoS ONE*, *8*(3), e58889.

Goldman, A. L., Van der Goes van Naters, W., Lessing, D., Warr, C. G., & Carlson, J. R. (2005). Coexpression of two functional odor receptors in one neuron. *Neuron*, *45*(5), 661–6.

Große-Wilde, E., Stieber, R., Forstner, M., Krieger, J., Wicher, D., & Hansson, B. S. (2010). Sex-specific odorant receptors of the tobacco hornworm *Manduca sexta*. *Frontiers in cellular neuroscience*, *4*(8), 1–7.

Guo, S., & Kim, J. (2010). Dissecting the molecular mechanism of drosophila odorant receptors through activity modeling and comparative analysis. *Proteins*, *78*(2), 381–99.

Hallem, E. a, & Carlson, J. R. (2006). Coding of odors by a receptor repertoire. *Cell*, *125*(1), 143–60.

Hildebrand, J. G. (1995). Analysis of chemical signals. *Proceedings of the National Academy of Sciences of the United States of America*, *92*(1), 67–74.

Hill, C. a, Fox, a N., Pitts, R. J., Kent, L. B., Tan, P. L., Chrystal, M. a, Cravchik, A., et al. (2002). G protein-coupled receptors in *Anopheles gambiae*. *Science (New York, N.Y.)*, *298*, 176–8.

Jarman, A. P. (2002). Studies of mechanosensation using the fly. *Human molecular genetics*, *11*(10), 1215–8.

Jones, P. L., Pask, G. M., Rinker, D. C., & Zwiebel, L. J. (2011). Functional agonism of insect odorant receptor ion channels. *Proceedings of the National Academy of Sciences of the United States of America*, *108*(21), 8821–5.

Jones, P. L., Pask, G. M., Romaine, I. M., Taylor, R. W., Reid, P. R., Waterson, A. G., Sulikowski, G. a, et al. (2012). Allosteric antagonism of insect odorant receptor ion channels. *PloS one*, *7*(1), e30304.

Kaissling, K. E., & Boekhoff, I. (1993). Transduction and intracellular messengers in pheromone receptor cells of the moth *Antheraea polyphemus*. *In: Arthropod Sensory Systems*. Wiese K, Gribakin FG, Popov AV, and Renninger G, eds., (pp. 489–502). Boston, Berlin: Birkhäuser Verlag Basel.

Kaissling, K., & Thorsen J. (1980). *Insect olfactory sensilla: structural, chemical and electrical aspects of the functional organization.* (D. Satelle, L. Hall, & J. Hildebrand, Eds.) (pp. 261–283). Amsterdam: Elsevier North-Holland Biomedical Press,.

Kaissling, K.-E. (2009). Olfactory perireceptor and receptor events in moths: a kinetic model revised. *Journal of comparative physiology. A, Neuroethology, sensory, neural, and behavioral physiology*, *195*(10), 895–922.

Kaupp, U. B. (2010). Olfactory signalling in vertebrates and insects: differences and commonalities. *Nature reviews. Neuroscience*, *11*(3), 188–200.

Keil, A. (1989). Fine structure of the pheromone-sensitive sensilla on the antenna of the hawkmoth, *Manduca sexta*. *Tissue and Cell*, *21*(1), 139–151.

Keil, A., & Steinbrecht, R. A. (1984). Mechanosensitive and olfactory sensilla of insects. In insect ultrastructure. (R. King & H. Akai, Eds.) (2nd ed., pp. 447–516). New York: Plenum.

Keil, T. (1993). Dynamics of immotile olfactory cilia in the silkmoth *Antheraea*. *Tissue and Cell*, *35*(4), 573–587.

Krause, T., Gerbershagen, M. U., Fiege, M., Weisshorn, R., & Wappler, F. (2004). Dantrolene--a review of its pharmacology, therapeutic use and new developments. *Anaesthesia*, *59*(4), 364–73.

Krieger, J, Klink, O., Mohl, C., Raming, K., & Breer, H. (2003). A candidate olfactory receptor subtype highly conserved across different insect orders. *Journal of comparative physiology. A, Neuroethology, sensory, neural, and behavioral physiology*, *189*(7), 519–26.

Krieger, Jurgen, Raming, K., Dewer, Y. M. E., Bette, S., Conzelmann, S., & Breer, H. (2002). A divergent gene family encoding candidate olfactory receptors of the moth *Heliothis virescens*. *European Journal of Neuroscience*, *16*(4), 619–628.

Larsson, M. C., Domingos, A. I., Jones, W. D., Chiappe, M. E., Amrein, H., & Vosshall, L. B. (2004). Or83b encodes a broadly expressed odorant receptor essential for Drosophila olfaction. *Neuron*, *43*(5), 703–14.

Laue, M., & Steinbrecht, R. A. (1997). Topochemistry of moth olfactory sensilla. *International Journal of Insect Morphology and Embryology*, *26*(3-4), 217–228.

Leal, W. S., Chen, A. M., Ishida, Y., Chiang, V. P., Erickson, M. L., Morgan, T. I., & Tsuruda, J. M. (2005). Kinetics and molecular properties of pheromone binding and release. *Proceedings of the National Academy of Sciences of the United States of America*, *102*(15), 5386–91.

Lee, J. K., & Strausfeld, N. J. (1990). Structure, distribution and number of surface sensilla and their receptor cells on the olfactory appendage of the male moth *Manduca sexta*. *Journal of neurocytology*, *19*(4), 519–38.

Lundin, C., Käll, L., Kreher, S. A., Kapp, K., Sonnhammer, E. L., Carlson, R., Heijne, G. Von, et al. (2007). NIH Public Access, *581*(29), 5601–5604.

Maida, R., Redkozubov, A., & Ziegelberger, G. (2000). Identification of PLC beta and PKC in pheromone receptor neurons of *Antheraea polyphemus*. *Neuroreport*, *11*(8), 1773–1776.

Malpel, S., Merlin, C., François, M.-C., & Jacquin-Joly, E. (2008). Molecular identification and characterization of two new Lepidoptera chemoreceptors belonging to the *Drosophila melanogaste*r OR83b family. *Insect molecular biology*, *17*(5), 587–96.

Nakagawa, Takao, & Vosshall, L. B. (2009). Mechanisms in the Insect Olfactory System, *19*(3), 284–292.

Nakagawa, Tatsuro, Pellegrino, M., Sato, K., Vosshall, L. B., & Touhara, K. (2012). Amino acid residues contributing to function of the heteromeric insect olfactory receptor complex. *PloS one*, *7*(3), e32372.

Neuhaus, E. M., Gisselmann, G., Zhang, W., Dooley, R., Störtkuhl, K., & Hatt, H. (2005). Odorant receptor heterodimerization in the olfactory system of *Drosophila melanogaster*. *Nature neuroscience*, *8*(1), 15–7.

Nichols, A. S., Chen, S., & Luetje, C. W. (2011). Subunit contributions to insect olfactory receptor function: channel block and odorant recognition. *Chemical senses*, *36*(9), 781–90.

Nolte, A. (2010). *Extrazelluläre Analyse der olfaktorischen Signaltransduktion beim Tabakschwärmer Manduca sexta*. Kassel.

Nolte, A., Funk, N. W., Mukunda, L., Gawalek, P., Werckenthin, A., Hansson, B. S., Wicher, D., et al. (2013). *In situ* Tip-Recordings Found No Evidence for an Orco-Based Ionotropic Mechanism of Pheromone-Transduction in *Manduca sexta*. *PLoS ONE*, *8*(5), e62648.

Olsson, S. B., Getahun, M. N., Wicher, D., & Hansson, B. S. (2011). Piezo controlled microinjection: an *in vivo* complement for in vitro sensory studies in insects. *Journal of neuroscience methods*, *201*(2), 385–9.

Parekh, B. (1997). Store Depletion and Calcium Influx. *Physiological Reviews*, *77*(4), 901–931.

Pask, G. M., Bobkov, Y. V, Corey, E. a, Ache, B. W., & Zwiebel, L. J. (2013). Blockade of insect odorant receptor currents by amiloride derivatives. *Chemical senses*, *38*(3), 221–9.

Pask, G. M., Jones, P. L., Rützler, M., Rinker, D. C., & Zwiebel, L. J. (2011). Heteromeric Anopheline odorant receptors exhibit distinct channel properties. *PloS one*, *6*(12), e28774.

Patch, H. M., Velarde, R. a, Walden, K. K. O., & Robertson, H. M. (2009). A candidate pheromone receptor and two odorant receptors of the hawkmoth *Manduca sexta*. *Chemical senses*, *34*(4), 305–16.

Pitts, R. J., Fox, a N., & Zwiebel, L. J. (2004). A highly conserved candidate chemoreceptor expressed in both olfactory and gustatory tissues in the malaria vector Anopheles gambiae. *Proceedings of the National Academy of Sciences of the United States of America*, *101*(14), 5058–63.

Putney, J. (2005). Capacitative calcium entry: sensing the calcium stores. *The Journal of cell biology*, *169*(3), 381–2.

Rogers, M E, Sun, M., Lerner, M. R., & Vogt, R. G. (1997). Snmp-1, a novel membrane protein of olfactory neurons of the silk moth *Antheraea polyphemus* with homology to the CD36 family of membrane proteins. *The Journal of biological chemistry*, *272*(23), 14792–9.

Rogers, Matthew E., Steinbrecht, R. a., & Vogt, R. G. (2001). Expression of SNMP-1 in olfactory neurons and sensilla of male and female antennae of the silkmoth *Antheraea polyphemus*. *Cell and Tissue Research*, *303*(3), 433–446.

Röllecke, K., Werner, M., Ziemba, P. M., Neuhaus, E. M., Hatt, H., & Gisselmann, G. (2013). Amiloride derivatives are effective blockers of insect odorant receptors. *Chemical senses*, *38*(3), 231–6.

Sanes, J. R., & Hildebrand, J. G. (1976a). Origin and morphogenesis of sensory neurons in an insect antenna. *Developmental biology*, *51*(2), 300–19.

Sanes, J. R., & Hildebrand, J. G. (1976b). Structure and Development of Antennae in a Moth , Manduca sexta, *299*, 282–299.

Sargsyan, V., Getahun, M. N., Llanos, S. L., Olsson, S. B., Hansson, B. S., & Wicher, D. (2011). Phosphorylation via PKC Regulates the Function of the Drosophila Odorant Co-Receptor. *Frontiers in cellular neuroscience*, *5*(6), 5.

Sasaki, M., & Riddiford, L. M. (1984). Regulation of reproductive behaviour and egg maturation in the tobacco hawk moth, *Manduca sexta*. *Physiological Entomology*, *9*(3), 315–327.

Sato, K., Pellegrino, M., Nakagawa, T., Nakagawa, T., Vosshall, L. B., & Touhara, K. (2008). Insect olfactory receptors are heteromeric ligand-gated ion channels. *Nature*, *452*(7190), 1002–6.

Shaw, G., Morse, S., Ararat, M., & Graham, F. L. (2002). Preferential transformation of human neuronal cells by human adenoviruses and the origin of HEK 293 cells 1, *16*(8), 869–871.

Simpson, P., Challiss, R. J., & Nahorski, S. (1995). Neuronal $Ca2^{+}$ stores : activation and function. *Trends Neuroscience*, *18*, 299–306.

Smart, R., Kiely, A., Beale, M., Vargas, E., Carraher, C., Kralicek, A. V, Christie, D. L., et al. (2008). Drosophila odorant receptors are novel seven transmembrane domain proteins that can signal independently of heterotrimeric G proteins. *Insect biochemistry and molecular biology*, *38*(8), 770–80.

Sonnhammer, E. L. L., Wistrand, M., & Ka, L. (2006). A general model of G protein-coupled receptor sequences and its application to detect remote homologs, 509–521.

Srikanth, S., & Gwack, Y. (2012). Orai1, STIM1, and their associating partners. *The Journal of physiology*, *590*(Pt 17), 4169–77.

Stengl, M. (1993). Intracellular-messenger-mediated cation channels in cultured olfactory receptor neurons. *The Journal of experimental biology*, *178*, 125–47.

Stengl, M. (1994). Inositol-trisphosphate-dependent calcium currents precede cation currents in insect olfactory receptor neurons *in vitro*. *Journal of comparative physiology. A, Sensory, neural, and behavioral physiology*, *174*(2), 187–94.

Stengl, M. (2010). Pheromone transduction in moths. *Frontiers in cellular neuroscience*, *4*(12), 133.

Stengl, M., & Funk, N. W. (2013). The role of the coreceptor Orco in insect olfactory transduction. *in review*.

Stengl, M., & Hildebrand, J. G. (1990). Insect olfactory neurons in vitro: morphological and immunocytochemical characterization of male-specific antennal receptor cells from developing antennae of male *Manduca sexta*. *The Journal of neuroscience : the official journal of the Society for Neuroscience*, *10*(3), 837–47.

Stengl, M., Zufall, F., Hatt, H., & Hildebrand, J. G. (1992). Olfactory receptor neurons from antennae of developing male *Manduca sexta* respond to components of the species-specific sex pheromone in vitro. *The Journal of neuroscience : the official journal of the Society for Neuroscience*, *12*(7), 2523–31.

Störtkuhl, K. F., & Kettler, R. (2001). Functional analysis of an olfactory receptor in Drosophila melanogaster. *Proceedings of the National Academy of Sciences of the United States of America*, *98*(16), 9381–5.

Suda, N., Franzius, D., Fleig, A., Nishimura, S., Bödding, M., Hoth, M., Takeshima, H., et al. (1997). $Ca2^{+}$-induced $Ca2^{+}$ release in Chinese hamster ovary (CHO) cells co-expressing dihydropyridine and ryanodine receptors. *The Journal of general physiology*, *109*(5), 619–31.

Syed, Z., & Leal, W. S. (2008). Mosquitoes smell and avoid the insect repellent DEET. *Proceedings of the National Academy of Sciences of the United States of America*, *105*(36), 13598–603.

Taylor, R. W., Romaine, I. M., Liu, C., Murthi, P., Jones, P. L., Waterson, A. G., Sulikowski, G. a, et al. (2012). Structure-Activity Relationship of a Broad-Spectrum Insect Odorant Receptor Agonist. *ACS chemical biology*.

Thurm, U., & Küppers, J. (1980). *Epithelial physiology of insect sensilla*. (M. Locke & D. Smith, Eds.) (Insect Bio., pp. 735–763). New York: Academic Press.

Tong, J., Du, G. G., Chen, S. R., & MacLennan, D. H. (1999). HEK-293 cells possess a carbachol- and thapsigargin-sensitive intracellular $Ca2^{+}$ store that is responsive to stop-flow medium changes and insensitive to caffeine and ryanodine. *The Biochemical journal*, *343 Pt 1*, 39–44.

Tripathy, S. J., Peters, O. J., Staudacher, E. M., Kalwar, F. R., Hatfield, M. N., & Daly, K. C. (2010). Odors Pulsed at Wing Beat Frequencies are Tracked by Primary Olfactory Networks and Enhance Odor Detection. *Frontiers in cellular neuroscience*, *4*(March), 1.

Tsitoura, P., Andronopoulou, E., Tsikou, D., Agalou, A., Papakonstantinou, M. P., Kotzia, G. a, Labropoulou, V., et al. (2010). Expression and membrane topology of *Anopheles gambiae* odorant receptors in lepidopteran insect cells. *PloS one*, *5*(11), e15428.

Tumlinson, J., Brennan, M., Doolittle, R., Mitchel, E., Brabham, A., Mazomenos, B., Baumhover, A., et al. (1989). Identification of a Pheromone Blend Attractive to Manduca sexta (L.) Males in a Wind Tunnel. *Archives of insect Biochemistry and Physiology*, *10*(4), 255–271.

Van Bambeke F, Barcia-Macay M, Lemaire S, & Tulkens PM. (2006). Cellular pharmacodynamics and pharmacokinetics of antibiotics : Current views and perspectives. *Opinion in Drug Discovery & Development*, *9*(2), 218–230.

Verkhratsky, a, & Shmigol, A. (1996). Calcium-induced calcium release in neurones. *Cell calcium*, *19*(1), 1–14.

Vosshall, L B, Amrein, H., Morozov, P. S., Rzhetsky, A., & Axel, R. (1999). A spatial map of olfactory receptor expression in the *Drosophila* antenna. *Cell*, *96*(5), 725–36.

Vosshall, L., Wong, A., & Axel, R. (2000). An olfactory sensory map in the fly brain. *Cell*, *102*(2), 147–59.

Vosshall, Leslie B, & Hansson, B. S. (2011). A unified nomenclature system for the insect olfactory coreceptor. *Chemical senses*, *36*(6), 497–8.

Wicher, D. (2013). Sensory receptors-design principles revisited. *Frontiers in cellular neuroscience*, *7*(January), 1. doi:10.3389/fncel.2013.00001

Wicher, D., Schäfer, R., Bauernfeind, R., Stensmyr, M. C., Heller, R., Heinemann, S. H., & Hansson, B. S. (2008). Drosophila odorant receptors are both ligand-gated and cyclic-nucleotide-activated cation channels. *Nature*, *452*(7190), 1007–11.

Wieczorek, H., Huss, M., Merzendorfer, H., Reineke, S., Vitavska, O., & Zeiske, W. (2003). The insect plasma membrane H^+ V-ATPase: intra-, inter-, and supramolecular aspects. *Journal of bioenergetics and biomembranes*, *35*(4), 359–66.

Wieczoreks, H., Putzenlechnere, M., & Klein, U. (1991). A Vacuolar-type Proton Pump Energizes. *The Journal of biological chemistry*, *266*(23), 15340–15347.

Woods, W. A., & Stevenson, R. D. (1996). Time and Energy Costs of Copulation for the Manduca sexta Sphinx Moth ,. *Phsiological Zoology*, *69*(3), 682–700.

Wybcrynski, R., Reagan, J., & Lerner, R. (1989). A Pheromone-Degrading Aldehyde Oxidase in the Antennae of the Moth *M. sexta*. *The Journal of neuroscience*, *9*(4), 1341–1353.

Yack, J. E. (2004). The structure and function of auditory chordotonal organs in insects. *Microscopy research and technique*, *63*(6), 315–37.

Yu, S. P., & Kerchner, G. A. (1998). Rapid Communication Endogenous Voltage-Gated Potassium Channels in Human Embryonic Kidney (HEK293) Cells, *617*(1), 612–617.

Ziegelberger, G., Van den Berg, M. J., Kaissling, K. E., Klumpp, S., & Schultz, J. E. (1990). Cyclic GMP levels and guanylate cyclase activity in pheromone-sensitive antennae of the silkmoths Antheraea polyphemus and Bombyx mori. *The Journal of neuroscience : the official journal of the Society for Neuroscience*, *10*(4), 1217–25.

Zwiebel, L. J., & Takken, W. (2004). Olfactory regulation of mosquito-host interactions. *Insect biochemistry and molecular biology*, *34*(7), 645–52.

8 Declaration of academic integrity

I, Sarah Körte, hereby declare, under oath, that this diploma thesis has been my independent work and has not been aided with any prohibited means. The terms “we” and “our” were solely used for linguistic reasons and do by no means signify the authorship of a second or third party. I declare, to the best of my knowledge and belief, that all passages taken from published and unpublished sources or documents, whether as original or slightly changed, have been mentioned as such at the corresponding places of this thesis by citation. My thesis has not been submitted for evaluation to another examination authority or has been published in this form or another.

Kassel, May 25th, 2013

.....

Sarah Körte